Preferred Conformers and Photochemical (λ > 200 nm) Reactivity of Serine and 3,3-Dideutero-Serine In the Neutral Form

S. Jarmelo,[†] L. Lapinski,[‡] M. J. Nowak,[‡] P. R. Carey,[§] and R. Fausto*,[†]

Department of Chemistry, University of Coimbra, 3004−535 Coimbra, Portugal, Institute of Physics, Polish Academy of Sciences, Al. Lotnikow 32/46, 02-668 Warsaw, Poland, and Department of Biochemistry, Case Western Reserve University, 10900 Euclid Ave., Cleveland Ohio 44106-4935

Received: March 4, 2005; In Final Form: April 22, 2005

A systematic investigation of the conformational potential energy surface of neutral serine [$HOCH_2CHNH_2$-COOH] and 3,3-dideutero-serine [$HOCD_2CHNH_2COOH$] was undertaken, revealing the existence of 61 different minima. The structures and vibrational spectra of the most stable conformers, which were estimated to have relative energies within 7 kJ mol^{-1} and account for ca. 93% of the total conformational population at room temperature, were calculated at both the MP2 and DFT/BLYP levels of theory with the 6-311++G-(d,p) basis-set and used to interpret the spectroscopic data obtained for the compounds isolated in low-temperature inert matrixes. The assignment of the main spectral infrared features observed in the range 4000−400 cm^{-1} to the most stable conformers of serine was undertaken. In addition, UV irradiation (λ > 200 nm) of the matrix-isolated compounds was also performed, leading to decarboxylation, which was found to be strongly dependent on the conformation assumed by the reactant molecule.

Introduction

Organic compounds observed in the interstellar medium and in solar system bodies are of particular importance for revealing the chemistry that may have led to life's origin and evolution.[1−5] Among these compounds, amino acids may have a crucial importance, since they are the basic components of proteins, which are the essential constituents of all organisms. Understanding the details of the structure of amino acids, under different experimental conditions, is then a fundamental problem in chemistry. On the other hand, the knowledge of the fundamental photochemical behavior of this type of compounds does also appear relevant to biochemistry and prebiotic chemistry.

Amino acids are well-known to exist in the zwitterionic form in the liquid or solid phases. Only very recently the neutral form of simple amino acids [glycine, sarcosine and *N*,*N*-dimethylglycine (DMG)] could be observed for the pure solid compounds, as a metastable species resulting from fast deposition of the gaseous compound onto a suitable substrate cooled at ca. 10 K.[6] The stabilization of the zwitterionic form in the condensed phases is essentially due to dipolar interactions and intermolecular H-bonds. On the contrary, in the gaseous phase, as well as for the compound isolated in low-temperature inert matrixes, amino acids exist in the neutral form. This has been confirmed for several amino acids, such as glycine, α- and β-alanine, proline, sarcosine, DMG, and γ-aminobutyric acid (GABA), by experimental studies based on microwave spectroscopy, electron diffraction and matrix-isolation infrared spectroscopy techniques.[6−14] In fact, for the isolated molecule situation, the zwitterionic species of simple amino acids have been shown not to constitute minimum energy structures, as revealed by high-level computational studies.[15,16]

The main obstacle to investigation of the neutral forms of amino acids is due to the difficulty of promoting sublimation of this kind of compound without significant decomposition. This results from the low vapor pressure shown by most of the amino acids at room temperature, due to the presence of very strong intermolecular H-bonds in the solid phase.

Serine is, among the simplest amino acids, one of those exhibiting lower vapor pressure and it decomposes extensively below its melting point, at normal pressure. Such behavior justifies the absence of any experimental study dealing with this amino acid in the gaseous phase. On the other hand, serine in the neutral form is a very interesting and challenging molecular system for structural research, because it contains a variety of intramolecular interactions. In particular, different types of H-bonds can be established between the various substituents in the molecule, leading to a large number of low energy conformers, stabilized by different intramolecular interactions.

Despite the relative complexity of serine, which is a conformationally flexible molecule with five internal rotation axes, several computational studies on this molecule have been reported previously.[17−29] However, with a single exception,[30] all studies have only considered a small subset of possible conformers.

Experimentally, amino acids have been extensively studied in their easily accessible zwitterionic form, but as mentioned above, they have been considerably less studied as neutral species. For instance, the photo- and thermal-decomposition behavior of neutral amino acid forms is a relatively recent topic of research.[31−33] In the case of serine, Zubavichus et al.[34] focused their attention on photodecomposition of the compound, as a solid layer adsorbed over indium, upon X-ray irradiation in ultrahigh vacuum. The experimental results indicated that the molecule decomposes by several pathways, such as dehydration, decarboxylation, decarbonylation, and deamination. On the other hand, Sato et al.[35] investigated the thermal decomposition of zwitterionic serine in water solution at high temperature (200−340 °C) and high pressure (MPa), concluding that the general

* Corresponding author. E-mail: rfausto@ci.uc.pt.
[†] University of Coimbra.
[‡] Polish Academy of Sciences.
[§] Case Western Reserve University.

10.1021/jp0511202 CCC: $30.25
Published on Web 06/09/2005

reaction network of amino acids under hydrothermal conditions takes two main paths: deamination to produce ammonia and organic acids and decarboxylation to produce carbonic acid and amines.

Neutral serine was for the first time successfully isolated in a low-temperature matrix in our laboratory, and preliminary results on the conformational preferences of this species were reported.[36,37] To sublimate efficiently the necessary amount of the compound without appreciable decomposition, we took advantage of the capabilities of the specially designed internal minifurnace developed in our laboratories for preparation of cryogenic matrixes of thermolabile low-vapor-pressure compounds.[38] Our experimental approach has been used later on by Lambie et al.,[29] to investigate the infrared spectrum of neutral serine isolated in solid argon. In that study, an assignment of the observed spectrum was proposed, which assumed significant contributions to the observed spectral features from the four conformers we had previously identified experimentally (Figure 1).[36,37] However, to undertake the band assignments, Lambie et al. relied only on the comparison between the experimental data and theoretical predictions of the vibrational spectra of the four conformers obtained at the DFT/B3LYP/6-31++G(d,p) level, not attempting to use any further information, such as, for example, those obtained by annealing or in situ irradiation of the matrix. These procedures can be expected to change the relative conformational populations and then enable a more reliable identification of bands due to each experimentally observable conformer. Furthermore, the possibility of contribution to the observed spectra of more than 4 conformers was not taken into consideration in that study.[29] As it will be shown in the present paper, this last assumption is in fact not supported by the experimental data.

In this work, the conformational preferences of neutral serine were studied, starting by a full systematic investigation of its potential energy surface. The optimized geometries and vibrational spectra of the 61 different conformers of serine and its 3,3-dideutero isotopologue were calculated, indicating that 9 conformers lay within 7 kJ mol^{-1} and account for ca. 93% of the total conformational population at room temperature. Theoretical calculations, undertaken at both the MP2 and DFT/B3LYP levels of theory with the 6-311++G(d,p) basis-set, together with temperature variation studies and in situ irradiation experiments were then used to interpret the spectroscopic data obtained for the compounds isolated in low-temperature inert matrixes. The assignment of the main spectral infrared features observed in the range 4000−400 cm^{-1} to the most stable conformers of serine was undertaken and the photochemical decarboxylation of both serine isotopologues, resulting from in situ UV irradiation ($\lambda >$ 200 nm) of the matrixes, was also investigated.

Materials and Methods

Computational Details. The theoretical calculations on serine and 3,3-dideutero-serine were performed with the Gaussian98 program package[39] at Hartree−Fock (HF), density functional theory (DFT), and second-order Møller−Plesset (MP2) levels of theory, with the standard split-valence 3-21G(d)[40−42] and extended 6-311++G(d,p)[43] basis sets. The DFT calculations were carried out with the three-parameter density functional abbreviated as B3LYP, which includes Becke's gradient exchange correction[44] and the Lee, Yang, and Parr correlation functional.[45] All structures were subjected to optimization without any geometrical constraints, and the resulting optimized geometries were characterized by inspection of the corresponding Hessian matrixes. Optimizations were followed by frequency calculations, performed at the same level of theory. The calculated frequencies were used to assist the analysis of the experimental spectra and to account for the zero-point vibrational energy (ZPVE) corrections. Due to the general good correspondence between the experimentally observed and the DFT/B3LYP/6-311++G(d,p) predicted spectra, these calculations were preferentially used both to assign the main features observed in the spectra of matrix-isolated monomers and to calculate energy barriers between the experimentally relevant conformers of serine. The DFT/B3LYP/6-311++G(d,p) harmonic frequencies and ZPVE were scaled using a single factor of 0.978,[46−48] except for νOH stretching modes, which were found to require the use of different scaling factors to describe properly the experimental spectra. For these vibrations, two scaling factors were used (0.953 or 0.913) depending on the strength of the H-bond interactions in which the corresponding hydroxyl group is involved.

Experimental Details. Both D,L-serine and its 3,3-dideuterated (>98% D) isotopologue used in this study were commercial products obtained from Aldrich and Icon Stable Isotopes, respectively. Matrixes were prepared by deposition of the vapor of the compounds onto a cold CsI (10 K) window directly assembled to the cold tip of a continuous flow liquid helium cryostat. The compounds were sublimated by electrical heating (470 K) in a specially designed minifurnace,[38] placed inside the vacuum chamber of the cryostat. The vapors of the compounds were deposited during ca. 70 min, together with a large excess of argon by Linde AG. T. These experimental conditions allowed minimization of trace amounts of thermal decomposition of the compound during sublimation. Argon of spectral purity (6.0) was supplied by Linde AG. The infrared spectra were recorded in the range 4000−400 cm^{-1}, with 0.5 cm^{-1} resolution and 600 scans, using a Thermo Nicolet Nexus 670 FTIR spectrometer equipped with KBr beam splitter and DTGS detector. Integral intensities of the IR absorption bands were measured by numerical integration. The matrixes were irradiated through the outer quartz window of the cryostat, using a high-pressure mercury lamp (HBO200) fitted with a water filter and a cutoff filter transmitting light with $\lambda >$ 200 nm. The time of irradiation was 30 min. After UV irradiation, the matrixes were annealed to 30 K.

Results and Discussion

Computational Results (Structures and Relative Conformational Energies). To truly characterize the conformations of serine, the full ensemble of possible conformations was considered. Preliminary calculations were undertaken at the less expensive HF level of theory, using the split-valence 3-21G(d) basis set. The starting set of serine conformations was chosen by allowing all possible combinations of single-bond putative rotamers (see Figure 2). There are five different internal rotation axes in serine that can give rise to conformational isomers. For the carboxyl group, internal rotation around the C(1)−O(3) bond leads to two possible minimum-energy arrangements: syn (τ(O(2)═C(1)O(3)H(4)) = 0°) and trans (τ(O(2)═C(1)O(3)H(4) = 180°). The orientation of the α-carbon substituents (NH_2 and CH_2OH) relative to the COOH group (internal rotation around the C_α−C(1) bond) can lead to six possible minimum-energy structures (corresponding to 3 staggered and 3 eclipsed geometries relative to the C═O bond). Both the NH_2 and CH_2-OH groups may adopt three different staggered arrangements (defined by the C_α−N and C_α−C_β internal rotations). Finally,

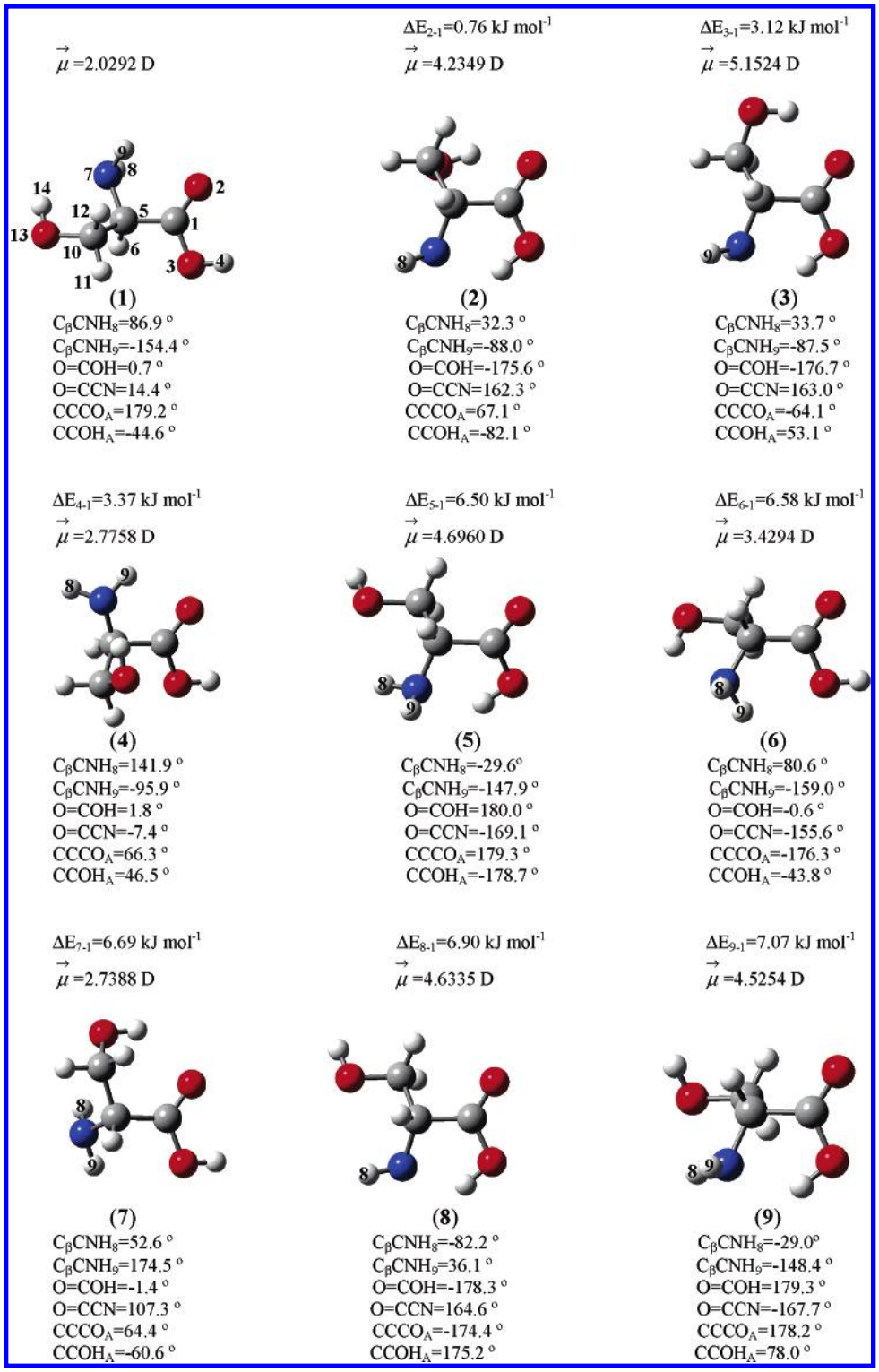

Figure 1. Nine most stable conformers of serine. Dihedral angles, dipole moments and energies presented in the Figure were obtained at the DFT/B3LYP/6-311++G(d,p) level. MP2/6-311++G(d,p) results are provided in the Supporting Information Table S1. Experimental observation of conformers 1−4 have been reported first in refs 33 and 34. In Figure S1 (Supporting Information), the nine conformers are represented in three alternative perspectives, for better viewing of some of the intramolecular interactions discussed in the text.

the C_β−O(13) bond represents a 3-fold rotor (Figure 2), defining the possible conformations of the OH_A group (throughout this article, in references to the OH groups, the subscript A stands for alcohol, whereas the subscript C stands for carboxylic group). All possible rotations around the axes described above lead to a total of 324 trial structures for the conformational states of serine, which were submitted to optimization. From the HF/3-21G(d) optimizations, 71 unique conformers were identified. These structures were afterward submitted to reoptimization at the DFT/B3LYP/6-311++G(d,p) level of theory.

At the DFT/B3LYP/6-311++G(d,p) level of theory, only 61 unique conformations were located, with energies varying by ≅47 kJ mol^{-1} (Table 1). Ten structures predicted at the HF/3-21G(d) level as minimum-energy conformations by the lower-level theory used were found to converge to other forms.

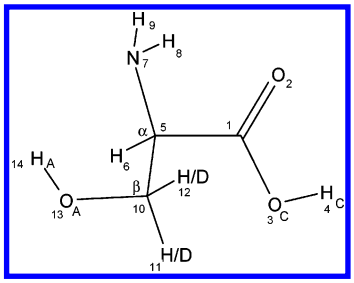

Figure 2. Atom numbering of serine/3,3-dideutero-serine. Internal rotation axes leading to possible rotamers: 2-fold, C(1)−C(3); 6-fold, C(1)−C(5); 3-fold, C(5)−N(7), C(5)−C(10), and C(5)−C(10). Subscripts A and C mean for "alcoholic" and "carboxylic".

Due to the very small differences in the relative conformational energies obtained at the DFT level, the energies of all conformers of serine predicted at this level of theory with energies within 7 kJ mol^{-1} were recalculated at the MP2/6-311++G(d,p) level of approximation (Table S1, Supporting Information), which usually estimates better this property than the DFT/B3LYP method with the same basis set.[49,50] The main difference between the results obtained with the two levels of theory relates to the relative energy of conformer **4** (see Figure 1 and Tables 1 and S1), which is predicted by the MP2 as lower than that obtained by the DFT calculations.

The relative energies shown in both Tables 1 and S1 suggest that the equilibrium mixture should contain significant contributions from several conformers, with the first nine (see Figure 1) playing the most important role. The relative populations of the nine most stable conformers, at $T = 470$ K (the temperature of the vapor immediately before deposition used in the matrix isolation experiments reported in this study), were predicted by the DFT calculations to be 1.00:0.74:0.28:0.26:0.07:0.07:0.07:0.06:0.06 [corresponding as a whole to 75% (21:17:9:9:4:4:4:4:3%) of the total conformational population]. [The relative populations predicted at the MP2 level are 1.00:0.63:0.09:0.55:0.07:0.08:0.06:0.03:0.04. Since at this level of theory only the energies of these nine conformers were calculated, no percent absolute populations can be given.]

As already mentioned, the presence of three H-bond donor and four H-bond acceptor groups in serine allows for a wide range of intramolecular interactions and, consequently, for a large number of stable conformations. For the purpose of systematically analyzing the large conformational data set studied, conformations were characterized by the H-bonds they exhibit. A distance of 2.7 Å was here used as a cutoff distance for H-bond interactions. This distance is consistent with typically values found in analogous systems with weak intramolecular H-bond interactions.[51] Although this approach is somewhat simplistic, it appears to be considerably more useful than a mere list of dihedral angles for illustrating the complex interactions found in the studied amino acid. It is worth mentioning the marked nonlinearity of intramolecular H-bonds, which leads to weakening of these interactions in serine.

The possible H-bonding schemes for serine are depicted schematically in Figure 3: **A**, COOH group in the cis conformation; OH_A group acting as proton-donor to the nitrogen atom. **B**, COOH group in the trans conformation; OH_C group acting as proton-donor to the nitrogen atom. **C**, COOH group in the cis conformation; OH_A group acting as proton-donor to the carbonyl oxygen. **D**, COOH group in the cis conformation; OH_A group acting as proton-donor to the O_C atom. **E**, COOH group in the cis conformation; NH_2 group acting as proton-donor to the carbonyl oxygen atom. **F**, COOH group in the cis conformation; NH_2 group acting as proton-donor to the O_A atom. **G**, COOH group in the cis conformation; NH_2 group acting as proton-donor to the O_C atom. **H**, COOH group in the trans conformation; OH_C group acting as proton-donor to the O_A atom. **I**, COOH group in the trans conformation; OH_A group acting as proton-donor to the carbonyl oxygen. **J**, COOH group in the trans conformation; OH_A group acting as proton-donor to the nitrogen atom. **K**, COOH group in the trans conformation; NH_2 group acting as proton-donor to the O_A atom. **L**, COOH group in the trans conformation; NH_2 group acting as proton-donor to the carbonyl oxygen atom. The H-bonding schemes appearing in each conformer of serine are given in Table 1. Note that associated with some of the H-bonding schemes there might also be a prevalence for occurrence of important steric repulsions, which may considerably destabilize the structures (e.g., in scheme **L**, the repulsion between OH_C and the hydrogen atoms of the methylene group; see Figure 3).

As a way of analyzing the general stability of the H-bonding schemes of serine, the average energies of the conformers within each scheme are compared with the overall mean energy in Table 2. The average energy of all conformers where the conformation of the carboxylic group is cis (37 conformers; see Table 1) was found to be 3.68 kJ mol^{-1} lower than the overall mean energy, whereas the corresponding value for the 24 conformers exhibiting a trans carboxylic group is larger than the global energy mean by 5.66 kJ mol^{-1}. These results show the general preference for the cis arrangement around the $C-O_C$ bond, as it is commonly found for unsubstituted carboxylic acids.[52−55] From the data shown in Table 2, it can also be concluded that in bonding schemes **A**−**H** the intramolecular attractive interactions are dominant, whereas in bonding schemes **I**−**L**, the repulsive interactions dominate.

As could be realized, serine can find stabilization via a variety of different combinations of the above considered H-bonding schemes. The nine most stable conformers differ in energy by less than ca. 7 kJ mol^{-1} and contain representatives of bonding schemes **A**−**C**. The first 44 conformers span less than 20 kJ mol^{-1}, and contain the entire characteristic set of bonding schemes (**A**−**L**).

Bonding scheme **A** (COOH group in the cis conformation; OH_A···N H-bond) is clearly more favorable than all of the remaining, justifying in large amount the greatest stability of conformer **1** and contributing also to the stabilization of conformers **4** and **6**.

The bonding scheme **B** is dominant in conformers **2**, **3**, **5**, **8**, and **9** which are stabilized by a strong OH_C···N hydrogen bonding interaction. In conformer **2**, the calculated OH_C···N distance is as short as 1.916 Å. On the other hand, to establish this H-bond, the conformation adopted by the carboxylic group in these conformers must be the less stable trans configuration.[52−55] However, the increase in energy due to the less stable geometry adopted by the carboxylic group is compensated by the establishment of a considerably strong H-bond, where the combination of donor and acceptor groups is the most favorable possible in serine.

Finally, conformer **7** reveals three different types of H-bonding schemes (**C**, **F** and **G**), with two of them (**C**, which is the dominant interaction, and **F**) existing only in this form (among the nine lowest energy conformers under analysis). Like in conformers **1**, **4** and **6**, the carboxylic group in this conformer adopts a cis conformation, but, instead of having the OH_A group acting as proton-donor to the nitrogen atom, this group establishes an H-bond with the carbonyl oxygen atom [scheme **C**; d(OH_A···O=)= 2.194 Å]. In addition, this conformer is also stabilized by two weaker H-bonds where the NH_2 group acts

TABLE 1: DFT/B3LYP/6-311++G(d,p) Calculated Dihedral Angles, Relative Energies ΔE^{ZPVE} [with Correction of Non-Scaled ZPVE] and Relative Populations at 298 and 470 K[a] of the Conformers of Serine

conformer	$C_\beta CNH_8$[b] (°)	$C_\beta CNH_9$ (°)	O=COH (°)	O=CCN (°)	$CCCO_A$ (°)	$CCOH_A$ (°)	E (kJ mol^{-1})	ZPVE (kJ mol^{-1})	E^{ZPVE} (kJ mol^{-1})	ΔE^{ZPVE} (kJ mol^{-1})[c]	population (%) 298 K	population (%) 470 K	H-bonding schemes[d]
1	86.9	−154.4	0.7	14.4	179.2	−44.6	−1047831.551	297.6457	−1047533.906	0.00	36.1	20.5	A/E
2	32.3	−88.0	−175.6	162.3	67.1	−82.1	−1047831.691	298.5456	−1047533.145	0.76	26.4	16.9	B/K
3	33.7	−87.5	-176.7	163.0	-64.1	53.1	−1047830.085	299.2947	−1047530.790	3.12	9.9	9.2	B/I
4	141.9	−95.9	1.8	−7.4	66.3	46.5	−1047828.035	297.4995	−1047530.535	3.37	8.9	8.7	A/E
5	−29.6	−147.9	180.0	−169.1	179.3	−178.7	−1047825.352	297.9462	−1047527.406	6.50	2.4	3.9	B/K
6	80.6	−159.0	-0.6	−155.6	−176.3	−43.8	−1047824.967	297.6457	−1047527.322	6.58	2.4	3.8	A/G
7	52.6	174.5	−1.4	107.3	64.4	−60.6	−1047825.222	298.0013	−1047527.220	6.69	2.3	3.7	C/F/G
8	−82.2	36.1	−178.3	164.6	−174.4	175.2	−1047824.449	297.4478	−1047527.001	6.90	2.1	3.5	B
9	−29.0	−148.4	179.3	−167.7	178.2	78.0	−1047825.105	298.2742	−1047526.831	7.07	1.9	3.4	B/K
10	56.7	173.9	1.4	−3.2	63.1	173.8	−1047821.437	296.1441	−1047525.293	8.61	1.0	2.3	E/F
11	66.4	−172.9	0.1	120.1	-57.9	69.9	−1047822.424	297.3426	−1047525.082	8.82	0.9	2.1	G
12	−88.9	29.7	−179.6	169.1	−175.3	87.4	−1047821.344	296.8667	−1047524.478	9.43	0.7	1.8	B/K
13	51.8	169.4	−2.2	−16.1	62.3	−83.9	−1047820.846	296.5127	−1047524.333	9.57	0.7	1.8	D/E
14	171.8	−68.2	−0.8	142.5	−66.4	65.5	-−1047820.736	297.1945	−1047523.541	10.36	0.5	1.4	C/G
15	152.7	−85.4	−1.3	174.5	69.9	44.6	−1047820.151	297.1617	−1047522.989	10.92	0.4	1.3	A/G
16	72.5	−170.0	0.0	2.2	−72.2	56.8	−1047819.435	296.4588	−1047522.976	10.93	0.4	1.3	D/E
17	152.0	−86.1	−0.1	−16.7	−74.8	63.4	−1047819.549	296.6436	−1047522.906	11.00	0.4	1.2	D/E
18	−175.9	−56.5	−1.8	134.2	−174.4	−171.3	−1047818.575	295.9719	−1047522.603	11.30	0.3	1.1	F/G
19	−83.1	36.1	−3.3	91.5	67.9	−62.4	−1047820.137	297.7695	−1047522.368	11.54	0.3	1.1	C/F
20	57.0	176.1	−1.4	−179.4	68.3	179.9	−1047817.893	296.3459	−1047521.547	12.36	0.2	0.9	F/G
21	137.2	−102.3	174.9	−14.3	−64.7	172.7	−1047818.496	297.2282	−1047521.267	12.64	0.2	0.8	H/L
22	−42.3	78.4	0.4	26.1	−179.0	−173.1	−1047816.962	295.7810	−1047521.181	12.72	0.2	0.8	E/F
23	−35.6	84.7	0.5	24.7	177.8	75.8	−1047817.396	296.4014	−1047520.994	12.91	0.2	0.8	E/F
24	170.0	-68.0	−0.6	−20.3	−173.6	−167.2	−1047816.336	295.534	−1047520.802	13.10	0.2	0.7	E/F
25	35.6	−87.7	−179.1	166.2	−169.8	−76.5	−1047817.714	297.1392	−1047520.575	13.33	0.1	0.7	B
26	52.8	176.1	0.6	−97.8	72.1	−65.0	−1047818.241	297.7322	−1047520.508	13.40	0.1	0.7	D/F
27	74.8	−166.5	3.5	−140.3	−51.6	−66.0	−1047816.547	296.3509	−1047520.196	13.71	0.1	0.6	E
28	74.9	−165.7	2.6	54.2	−58.0	169.8	−1047815.802	295.9148	−1047519.887	14.02	0.1	0.6	E
29	−40.4	83.1	−0.4	15.3	−74.4	53.7	−1047815.381	296.0383	−1047519.343	14.56	0.1	0.5	D/E
30	139.9	−99.3	174.5	−17.4	−61.1	−85.9	−1047815.501	297.2116	−1047518.289	15.62	0.1	0.4	H/L
31	−54.3	67.5	0.5	−179.5	−67.5	51.7	−1047815.022	296.8826	−1047518.140	15.77	0.1	0.4	C/G
32	173.7	−63.0	−0.2	−17.0	−176.1	81.5	−1047813.311	295.4638	−1047517.847	16.06	0.0	0.3	E/F
33	70.5	−169.1	−1.9	−121.8	−48.8	−66.5	−1047814.021	296.2316	−1047517.789	16.12	0.0	0.3	G
34	−173.4	−52.7	-2.0	136.6	−176.5	80.9	−1047813.096	295.6976	−1047517.399	16.51	0.0	0.3	F/G
35	−52.0	67.1	1.9	−146.2	−174.8	−176.0	−1047812.592	295.6610	−1047516.931	16.97	0.0	0.3	F/G
36	−47.0	71.6	1.6	−148.4	−177.0	78.7	−1047812.975	296.1574	−1047516.818	17.09	0.0	0.3	F/G
37	71.9	−167.5	−1.3	−107.9	−55.2	173.0	−1047812.601	295.8302	−1047516.771	17.13	0.0	0.3	G
38	164.0	−77.8	176.0	−86.7	62.0	52.7	−1047815.990	299.3557	−1047516.635	17.27	0.0	0.2	H/J/L
39	−42.9	77.0	1.5	14.3	60.6	−179.2	−1047811.444	294.9948	−1047516.449	17.46	0.0	0.2	E/F
40	−50.0	70.9	2.4	44.1	−57.3	−61.6	−1047811.609	295.9102	−1047515.699	18.21	0.0	0.2	E
41	−60.6	60.7	0.8	61.1	−63.2	167.0	−1047810.846	295.4981	−1047515.348	18.56	0.0	0.2	E
42	−58.6	60.4	−1.0	-167.5	67.5	−173.5	−1047810.148	295.6005	−1047514.548	19.36	0.0	0.1	F
43	−163.6	−44.7	−178.5	−162.5	60.0	59.3	−1047812.077	297.6456	−1047514.431	19.47	0.0	0.1	B/J
44	−64.2	59.7	1.9	−143.6	−176.1	−77.7	−1047809.706	295.3557	−1047514.350	19.56	0.0	0.1	e
45	−61.8	59.2	0.2	−126.3	−51.7	−60.2	−1047808.461	295.5457	−1047512.916	20.99	0.0	0.1	G
46	86.7	−155.4	−178.1	16.8	−179.5	−46.0	−1047807.716	296.4969	−1047511.219	22.69	0.0	0.1	J/L
47	−67.0	54.6	0.8	−115.1	−58.3	171.6	−1047805.625	295.0778	−1047510.547	23.36	0.0	0.1	G
48	−90.0	148.5	172.8	−19.1	62.1	46.3	−1047803.188	296.5185	−1047506.670	27.24	0.0	0.1	J/L
49	−176.2	−57.3	−0.9	−109.3	−57.9	−65.3	−1047801.585	295.5773	−1047506.007	27.90	0.0	0.0	e
50	179.2	-61.5	-1.2	107.5	−72.6	−70.1	-1047800.876	295.4302	−1047505.446	28.46	0.0	0.0	G
51	-78.1	43.1	-171.4	−103.2	67.7	−175.0	−1047800.389	296.3958	−1047503.994	29.91	0.0	0.0	K
52	49.3	170.8	175.8	91.3	66.0	−63.1	−1047799.607	297.2640	−1047502.343	31.56	0.0	0.0	I/K
53	43.7	−77.2	−174.4	156.0	−75.7	−67.0	−1047797.804	296.4284	−1047501.376	32.53	0.0	0.0	B
54	−42.3	78.0	−174.6	38.0	−177.6	−169.0	−1047794.188	294.9467	−1047499.241	34.66	0.0	0.0	K/L
55	59.2	175.4	176.6	−7.0	60.1	165.1	−1047794.171	294.9798	−1047499.192	34.71	0.0	0.0	K/L
56	77.4	−161.8	−175.6	−93.6	−177.0	−41.6	−1047793.509	296.7026	−1047496.806	37.10	0.0	0.0	J
57	−34.8	85.1	−174.1	33.8	176.4	76.3	−1047791.608	295.1318	−1047496.476	37.43	0.0	0.0	K/L
58	160.5	−75.9	−178.4	−8.7	−171.8	−157.1	−1047790.114	293.9490	−1047496.165	37.74	0.0	0.0	K/L
59	167.5	−67.5	179.4	−13.4	−176.7	74.7	−1047784.412	294.0524	−1047490.359	43.55	0.0	0.0	K/L
60	−29.5	90.9	−176.4	16.6	59.4	177.4	−1047783.446	293.3753	−1047490.071	43.83	0.0	0.0	L
61	68.3	−170.1	179.0	−100.7	−57.3	67.4	−1047781.707	294.6814	−1047487.025	46.88	0.0	0.0	e

[a] 470 K, sublimation temperature used during the deposition process in the matrix isolation experiments. [b] See Figure 2 for atom numbering. [c] For the nine most stable conformers, ΔE^{ZPVE} values calculated at the MP2/6-311++G(d,p) level are 0.00, 1.13, 5.88, 1.46, 6.47, 6.13, 7.03, 8.43, and 7.98 kJ mol^{-1} (see also Table S1). [d] In the last column the H-bonding schemes for the corresponding conformer are indicated (see text). See Figure 3 for H-bonding schemes labeling. [e] Conformers **61**, **44,** and **49** of serine do not show any intramolecular hydrogen bond.

as proton-donor: $NH_{(8)}\cdots O_A$ (scheme **F**) and $NH_{(9)}\cdots O_C$ (bonding scheme **G**).

As general conclusions, from the data shown in Table 2 (and also in Table 1), the following can be stated:

(a) The cis arrangement of the carboxylic group is preferred over the trans configuration (with a single exception, **B**, all preferred bonding schemes have the carboxylic group in the cis conformation).

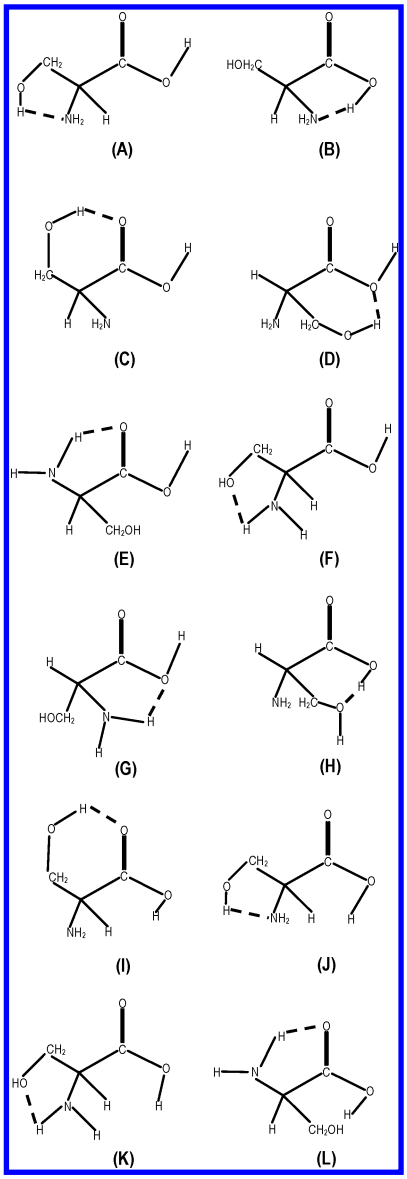

Figure 3. H-bonding schemes for serine.

TABLE 2: Average Energy (AE_Γ) of the Conformers of Serine with H-Bonding Scheme Γ[a]

H-bond schemes (Γ)	AE_Γ[b] (kJ mol^{-1})	AE_Γ-AE_A (kJ mol^{-1})	AE_Γ-$\overline{AE}$ (kJ mol^{-1})
A	−1047528.7	0.0	−10.8
B	−1047522.9	5.8	−5.0
C	−1047522.8	5.9	−4.9
D	−1047522.0	6.7	−4.1
E	−1047521.7	7.0	−3.8
F	−1047520.2	8.5	−2.3
G	−1047518.9	9.8	−1.0
H	−1047518.7	10.0	−0.8
I	−1047516.6	12.1	1.3
J	−1047509. 2	19.5	8.7
K	−1047508.5	20.2	9.4
L	−1047504.1	24.5	13.8

[a] AE_A is the average energy of serine conformers with H-bonding scheme A. AE is the average energy of all conformers of serine. [b] All energies were calculated at DFT/B3LYP/6-311++G(d,p) level, with ZPVE correction taken into account.

(b) The interaction of the carboxyl proton with the hydroxyl side chain (bonding scheme **H**) is less favorable than those with nitrogen (bonding scheme **B**).

(c) When acting as donor group, the alcohol group (OH_A) prefers to take part in H-bonding interactions with the nitrogen atom (scheme **A**) or with the carbonyl oxygen atom (scheme **C**) than with O_C (scheme **D**). This trend correlates well with the increase in the basicity of the acceptor group along the series O_C, O=, N.

(d) In general, the H-bonding schemes where either the OH_C or OH_A groups act as the donating group are preferred over those where the NH_2 group takes this role (thus, schemes **A**, **C** and **D** are preferred over **E**, **F** and **G**, and schemes **H**, **I** and **J** are preferred over **K** and **L**).

(e) The conjugation of better donating (OH_C) and acceptor (N) moieties occurs in scheme **B**, justifying the exceptional character of the position occupied by this bonding scheme (which is associated with the higher-energy trans arrangement of the carboxylic group, but corresponds to the second preferred structural arrangement) in the energy scale.

(f) taking into consideration the dominant intramolecular interactions in the nine most stable conformers of serine, they can be grouped in 3 classes: **1**, **4** and **6**, where bonding scheme **A** dominates; **2**, **3**, **5**, **8** and **9**, where bonding scheme **B** is prevalent and **7**, where the most relevant interaction is **C**.

It is also worth noting that the different types of structures exhibited by the nine most stable conformers of serine are reflected in their geometrical parameters (see Table S2, provided as Supporting Information). For instance, the C=O and C−O_C bonds are systematically longer (by ∼0.003 and ∼0.02 Å, respectively) and the C−C_α and C_α−N bonds are shorter (by 0.01−0.02 Å) in conformers where the carboxyl group adopts the cis conformation, relative to those where the same group assumes the trans orientation. On the other hand, the involvement of the carbonyl oxygen in the OH_A···O= hydrogen bond in both forms **3** and **7** can easily be correlated with the longer C=O distances observed for these two conformers (indeed, regarding the C=O bond length, conformer **3**, which has a trans carboxylic group is the exception relative to the above-mentioned trend which states that this bond length should be longer for conformers with cis carboxylic groups than for those with a trans carboxylic group). Furthermore, accordingly to the involvement in the strong OH_C···N hydrogen bond, the OH_C bond attains its maximum length in conformers **2**, **3**, **5**, **8**, and **9** (longer by ca. 0.14 Å than in the other conformers), whereas the OH_A bond is consistently longer in the conformers where this group acts as H-bond donor (**1**, **3**, **4**, **6**, and **7**) than in the remaining conformers.

The distinction between the cis and trans carboxylic conformers of serine can also be clearly noticed in the calculated dipole moments (see Figure 1). The trans conformers (**2**, **3**, **5**, **8**, and **9)** exhibit a systematically higher dipole moment (ca. 4−5 D) than the cis forms (ca. 2−3 D).

Spectroscopic Results (Supported by Calculated IR Spectra and Energy Barriers to Conformational Isomerization). As discussed in detail above, the calculated relative energies (see Table 1) suggest that in the gas-phase-equilibrium the conformational mixture shall contain relevant contributions from the nine most stable conformers of serine. Assuming that the relative populations of serine conformers frozen into a low-temperature matrix should correspond to gas-phase equilibrium, the matrix-isolation infrared (MI−IR) spectroscopy technique could provide a suitable way to experimentally test the theoretical predictions, since the different conformers of serine shall give rise to distinguishable MI−IR spectra (see Tables S3−S21, provided as Supporting Information).

As already mentioned, the set of nine most stable conformers of serine can be divided into three groups (group **A**, conformers **1**, **4**, and **6**; group **B**, **2**, **3**, **5**, **8**, and **9**; and group **C**, **7**). In each of these groups, there are common structural characteristics that can be expected to be relevant in determining the vibrational signature of its elements, in particular in the spectral regions corresponding to vibrations that can be expected to be most affected by H-bond interactions. To facilitate discussion of the assignment of the infrared spectra of D,L-serine and D,L-3,3-dideutero-serine, the analysis will be performed by dividing the spectra into different regions. Only the most representative spectral regions will be discussed in detail in the forthcoming sections. Tables 3 and 4 summarize the proposed assignments for these two molecules and compare the experimentally observed frequencies with those obtained theoretically at the DFT/B3LYP/6-311++G(d,p) level for the relevant conformers.

νOH and νNH_2 Stretching Region (3700−3100 cm^{-1}). In this spectral region, the theoretical calculations predict that all conformers of practical relevance should give rise to bands due to νNH_2 stretching modes (both symmetric and antisymmetric). These bands are of low intensity and lie at nearly the same position (νNH_2 asym: 3498−3528 cm^{-1}; νNH_2 sym: 3418−3440 cm^{-1}; see Tables 3 and 4 and Figure 4). Experimentally, the features ascribable to the antisymmetric mode are observed between 3500 and 3540 cm^{-1} and those due to the symmetric mode between 3390 and 3440 cm^{-1}, in good agreement with the theory. On the other hand, the bands due to νOH stretching vibrations were predicted to appear at considerably different frequencies in the three groups of conformers (see Figure 4). In conformers belonging to group **A**, the νOH_C bands are predicted to occur at slightly higher frequencies than νOH_A, since in these conformers the alcohol group is H-bonded to the amine group. The predicted frequency for νOH_C is typical of a free cis carboxylic group and is considerably lower than those of the free alcohol groups in all conformers of group **B** but conformer **3** (where OH_A is H-bonded to the carbonyl oxygen; see Figure 1). In conformer **7** (group **C**), the predicted order of frequencies for the νOH_C and νOH_A modes is reversed, since in this case the H-bond involving the alcohol group is established with the carbonyl oxygen atom, which is a weaker H-bond acceptor than the amine nitrogen. Despite the change in the order of the two νOH stretching modes in groups **A** and **C**, the general pattern of the spectra for all conformers belonging to these two groups is predicted to be identical (see Figure 4). In conformers belonging to group **B**, where the alcohol group is free, νOH_A is predicted at frequencies above 3600 cm^{-1} (scaled values; the exception is conformer **3** where, as mentioned above, the OH_A group is H-bonded to the carbonyl oxygen and then gives rise to a νOH_A vibration with a frequency similar to those found in groups **A** and **C**), whereas νOH_C is predicted at considerably lower frequencies, due to the involvement of the carboxylic group in the strong $OH_C \cdots NH_2$ hydrogen bond (see Figure 4). In consonance with these predictions, in the spectra of D,L-serine and D,L-3,3-dideutero-serine in an argon matrix the "free" νOH_A bands of **B** conformers **2**, **9**, **5**, and **8** are observed at 3629, 3637, 3660, and 3664 cm^{-1}, respectively, whereas those corresponding to the H-bonded OH_A group in **C** and **A** conformers appear at 3610 cm^{-1} and in the 3560−3550 cm^{-1} region, respectively (the νOH_A band of conformer **3** is observed at 3543 cm^{-1}). In turn, the "free" νOH_C vibrations in conformers belonging to groups **A** and **C** give rise to the bands observed at 3592 (form **4**), 3585 (**6**), 3567 (**1**), and 3564 (**7**) cm^{-1}, whereas those originated in the strongly H-bonded carboxylic group of **B** conformers can be ascribed to the broad band centered around 3170 cm^{-1}.

It is important to note that it was possible to identify bands in this spectral region ascribable to each one of the nine conformers of serine that are predicted by the theory to contribute in significant amounts to the conformational equilibrium at the temperature used for evaporation of serine during deposition of low-temperature matrixes.

To change the relative populations of the conformers trapped in the matrix and allow for a more clear assignment of the bands to the different conformers, UV irradiation (λ > 200 nm) of the sample followed by annealing up to 30 K was undertaken. The following processes were observed to occur:

(i) Upon UV irradiation of the matrixes, decarboxylation of serine was observed, as easily noticed by the appearance of features due to matrix isolated CO_2, around 2340 cm^{-1} (antisymmetric stretching) and 668 cm^{-1} (bending). The photoproducts of serine decarboxylation (CO_2 and other photogenerated species) are confined in the same matrix cage. The interaction between these photoproducts is revealed by the broad profile of the antisymmetric stretching band, which differs considerably from that characteristic of monomeric CO_2 in an argon matrix[56] (Figure 5).

(ii) With all probability, ethanolamine is produced together with CO_2. However, the complexity of the spectra, together with the low intensity of the bands of ethanolamine comparatively to those of serine (the most intense band of ethanolamine lying in the accessible spectral region was predicted at the DFT-(B3LYP)/6-311++G(d,p) level of theory to have an IR intensity of only ca. 100 km mol^{-1}, whereas the most intense bands of serine have IR intensities over 300 km mol^{-1}), the possibility of photoproduction of different conformers of ethanolamine (absorbing at slightly different frequencies), and the relatively low efficiency of the photoprocess, preclude a clear identification of this compound in the spectra of the irradiated matrixes. In the high frequency (νOH stretching) region of the IR spectrum, the most stable conformer of ethanolamine isolated in an Ar matrix absorbs at 3555 cm^{-1},[57] which coincides exactly with the frequency of the most intense group of bands observed in this spectral region for serine. A band, appearing in the high-frequency range of the IR spectrum upon UV irradiation of the matrix, is observed at 3624 cm^{-1} (at the same frequency in the spectra of irradiated serine and irradiated deuterated serine). This band might correspond to ethanolamine complexed with CO_2, but this assignment must be considered as tentative. In addition, there are also new bands at 3726 and 3701 cm^{-1}. These bands might be ascribed to water appearing after irradiation. Water can be formed together with carbon monoxide and acetamide. Identification of a small amount of CO could be easily done, since its characteristic band at 2138 cm^{-1} was also observed in the spectrum of the irradiated sample. On the other hand, no conclusive identification of acetamide could be made, because this molecule absorbs in spectral regions where intense bands due to serine appear and, as inferred by the intensity of the bands at 3726 and 3701 cm^{-1} as well as that ascribed to CO, the dehydration reaction was of minor importance.

(iii) During UV irradiation, the decrease of intensity of the bands ascribed to the different conformers of serine occurs at different rates. Among the nine conformers experimentally observed, conformer **7** (**C** conformer) is the one that reacts faster, followed by **A**-type conformers (conformers **1**, **4**, and **6**). This means that the photodecarboxylation is strongly influenced by the conformation of the reactant molecule,

TABLE 3: Calculated DFT/B3LYP/6-311++G(d,p) for the Nine Most Stable Conformers of D,L-Serine and Experimental MI-IR Spectrum (Argon)

	1		2		3		4		5		6		7		8		9		exptl	
approx. descript.[a]	freq.$_{scal}$[b] (cm^{-1})	int.	freq.$_{scal}$[b] (cm^{-1})	int.	freq.$_{scal}$[b] (cm^{-1})	int.	freq.$_{scal}$[b] (cm^{-1})	int.	freq.$_{scal}$[b] (cm^{-1})	int.	freq.$_{scal}$[b] (cm^{-1})	int.	freq.$_{scal}$[b] (cm^{-1})	int.	freq.$_{scal}$[b] (cm^{-1})	int.	freq.$_{scal}$[b] (cm^{-1})	int.	freq. (cm^{-1})	int.[c]
νOH_A															3669.8	48			3664	w
νOH_A									3667.6	52									3660	w
νOH_A																	3651.1	42	3637	w
νOH_A			3640.3	48															3629	w
νOH_A													3601.8	66					3610	w
νOH_C							3585.9	83											3592	w
νOH_C											3579.9	79							3585	sh
νOH_C	3573.8	68																	3567	m
νOH_C													3570.4	74					3564	m
νOH_A							3552.3	62			3555.6	70							3560	m
νOH_A	3551.3	73																	3556; 3551	s; sh
νOH_A					3545.0	137													3543	sh
νNH_2 as.	3505.6	13	3509.8	16	3513.8	13	3527.9	23	3498.0	22	3515.4	12	3517.6	13	3507.8	12	3499.2	21	3518	sh
νNH_2 s.							3439.7	13			3437.9	5							3427	w
νNH_2 s.					3428.1	25			3431.4	2			3430.0	4			3429.9	4	3418	w
νNH_2 s.	3425.5	7													3425.0	7			3413	w
νNH_2 s.			3418.0	16															3404	w
νOH_C			3163.3	276	3184.3	236			3155.5	292					3174.8	274	3168.4	274	≅3170	vb
νCH_2 as.	3038.5	18	3029.8	17			3045.5	15			3035.9	18	3036.9	17			3033.5	16	2983	w
$\nu C_\alpha H$											3018.1	5								
$\nu C_\alpha H$	3004.8	7																		
νCH_2 as.					3004.0	29			3008.2	21					3008.3	18				
νCH_2 s.			2984.9	38													2983.5	19	2950; 2940	w; w
$\nu C_\alpha H$			2970.2	6	2982.1	11			2976.3	13			2972.9	29	2977.6	6	2952.9	20		
νCH_2 s.													2949.2	37						
$\nu C_\alpha H$							2922.8	69											2888;	w;
νCH_2 s.	2904.3	52			2895.5	58	2910.0	35	2931.7	32	2905.1	54			2916.9	44			2866	w
$\nu C{=}O$									1795.3	353					1792.6	341	1793.6	349	1790; 1788	sh; s
$\nu C{=}O$			1785.8	328															1778	sh
$\nu C{=}O$	1766.4	315			1771.6	310													1773	vs
$\nu C{=}O$	1766.4	315					1769.5	304			1769.7	317							1771	vs
$\nu C{=}O$													1744.8	305					1755	s
δNH_2	1633.4	35	1616.6	37	1622.8	37	1601.2	71	1631.3	38	1628.9	37	1609.7	40	1631.4	37	1630.5	37	1646; 1600; 1560; 1527	w; w; w; w
δCH_2	1478.9	2			1474.9	2	1475.9	3	1481.7	5	1478.3	2			1483.2	3			1473	w
δCH_2			1460.0	7									1461.1	6			1467.9	4	1457	w
δCOH_A					1418.6	20														
ωCH_2									1412.4	3					1408.5	3			1410	sh
ωCH_2							1401.7	43												
δCOH_A	1401.1	66									1399.2	65	1398.7	24						
$\rho C_\beta C_\alpha H$	1392.3	9					1389.3	27											1400;	s;
δCOH_C			1390.7	295					1387.2	380					1384.6	404	1384.0	225	1384	m
ωCH_2																	1379.2	179		
δCOH_C					1376.2	468													1376	m
$\rho C_\beta C_\alpha H$											1376.1	18								
$\rho C_\beta C_\alpha H$															1372.4	10				
$twCH_2$			1370.4	117															1371	sh
ωCH_2			1365.5	21																
$\delta C_\beta C_\alpha H$													1364.4	19					1367	sh
ωCH_2													1360.4	3						
$\rho C_\beta C_\alpha H$					1359.3	11													1360	sh
$twCH_2$																	1353.6	9		
ωCH_2					1347.0	13														
$\rho C_\beta C_\alpha H$			1346.4	16									1347.6	39					1345	w
ωCH_2	1342.0	1																		
$\rho C_\beta C_\alpha H$									1341.4	28										
δCOH_A							1338.6	5												
ωCH_2											1338.4	11							1328	w
$\rho C_\beta C_\alpha H$																	1334.0	28		
δCOH_C; $\nu C\text{-}O_C$											1309.8	30								
δCOH_C	1304.1	46																		
δCOH_C							1295.1	26												
ρNH_2									1292.7	<1										
$\delta C_\beta C_\alpha H$					1284.5	5									1285.3	11			1305;	w;
δCOH_C													1274.1	5					1291;	sh;
$\delta C_\beta C_\alpha H$			1271.7	6													1271.2	1	1279;	m;
$twCH_2$									1271.2	4									1266	m
$\delta C_\beta C_\alpha H$							1266.9	4												
ρNH_2	1260.3	11															1260.8	9		
ρNH_2											1255.3	29								
$\delta C_\beta C_\alpha H$											1250.6	3								
$twCH_2$															1243.3	3				

TABLE 3 (Continued)

	1		2		3		4		5		6		7		8		9		exptl	
approx. descript.[a]	freq.-scal[b] (cm^{-1})	int.	freq.-scal[b] (cm^{-1})	int.	freq.-scal[b] (cm^{-1})	int.	freq.-scal[b] (cm^{-1})	int.	freq.-scal[b] (cm^{-1})	int.	freq.-scal[b] (cm^{-1})	int.	freq.-scal[b] (cm^{-1})	int.	freq.-scal[b] (cm^{-1})	int.	freq.-scal[b] (cm^{-1})	int.	freq. (cm^{-1})	int.[c]
$\delta C_\beta C_\alpha H$	1229.3	8																		
$twCH_2$													1215.9	14						
δCOH_A									1210.7	29									1229;	w;
δCOH_A			1205.1	15											1206.5	26			1218;	w;
$\delta C_\beta C_\alpha H$									1200.0	5									1203;	w;
$twCH_2$					1196.2	8	1195.8	22											1190;	sh;
$\nu C\text{-}O_C$					1191.8	28													1183	sh
ρNH_2							1188.0	45												
$\nu C\text{-}O_C$																	1185.5	18		
$\nu C\text{-}O_C$			1182.1	24											1182.0	17				
ρNH_2													1164.1	1						
$twCH_2$											1161.0	43							1168	sh
ρNH_2															1160.8	4				
$\nu C\text{-}O_C$									1160.6	21									1163	m
$twCH_2$	1157.4	55																	1150	m
ρNH_2					1157.0	6														
ρNH_2			1148.7	6															1141	sh
$\nu C\text{-}O_C$	1135.1	84																	1137	s
$\nu C\text{-}O_C$							1131.8	174											1132	sh
δCOH_C; $\nu C\text{-}O_C$											1129.8	203							1126	sh
$\nu C\text{-}O_C$													1121.7	317					1123	m
δCOH_A																	1110.6	23		
$\nu N\text{-}C$											1102.8	10							1113;	sh;
$\nu N\text{-}C$	1096.0	148			1087.4	8	1092.6	85					1098.2	49			1091.9	35	1105	vs
$\nu N\text{-}C$									1081.6	39					1084.5	47			1101;	sh;
																			1098;	sh;
																			1092	sh
$\nu C_\alpha C_\beta$			1077.0	63															1073	sh
ρCH_2															1060.5	25				
$\nu C\text{-}O_A$	1058.0	144			1059.4	101					1057.3	133							1065	s
ρCH_2			1051.1	17															1057	m
$\nu C\text{-}O_A$							1050.8	88												
$\nu C\text{-}O_A$									1034.1	95							1034.4	130	1043;	sh;
																			1030	sh
$\nu C\text{-}O_A$													1028.1	9					1018;	sh;
																			1013	w
$\nu C_\alpha C_\beta$					1026.0	59														
$\nu C\text{-}O_A$															1019.1	111			1010	w
ρCH_2	996.2	3							999.0	38									995;	w;
ρCH_2											986.5	3	984.6	59					992	w
ρCH_2					971.1	14	978.4	2									973.6	38	977	m
$\nu C\text{-}O_A$			963.9	82															975;	m;
																			974;	sh;
																			973	sh
ωNH_2									939.8	81					939.7	59			948	sh
ωNH_2																	925.5	57	932;	w;
$\nu C_\alpha C$	921.4	59																	926	sh
ωNH_2			913.7	73															914	w
$\nu C_\alpha C$											897.7	99							904;	w;
$\nu C_\alpha C_\beta$							890.7	26					891.8	5					897	sh
$\nu C_\alpha C_\beta$	872.0	38							872.0	57	870.5	21							884;	sh;
																			873;	w;
																			871	sh
$\nu C_\alpha C_\beta$															866.2	73	863.2	66	860;	m;
ωNH_2							864.4	92											858	sh
$\tau C\text{-}O_C$			861.7	61	856.9	88			854.1	71							848.1	33		
$\nu C_\alpha C$									841.1	21					842.1	43	837.5	62		
$\nu N\text{-}C$			838.9	101															845	m
$\tau C\text{-}O_C$															833.3	68				
ωNH_2													828.4	89					832	sh
ωNH_2	825.2	119			823.9	130													827;	m;
																			822;	m;
																			817;	s;
																			814	sh
ωNH_2											805.0	114							808;	w;
																			803;	w;
γCOO			798.0	11			798.6	64					803.2	74					800;	sh;
																			793;	w;
$\nu C_\alpha C$					789.3	16													790;	sh;
																			785;	m;
																			783	sh
$\delta C{=}O$			752.5	7															773	w
$\nu C_\alpha C$							736.9	33					734.6	41					766	w
γCOO	719.5	29			723.8	8					726.7	27			719.3	10			748;	m;
																			747;	sh;
																			744	sh

TABLE 3 (Continued)

	1		2		3		4		5		6		7		8		9		exptl	
approx. descript.[a]	freq.$_{\cdot scal}$[b] (cm^{-1})	int.	freq.$_{\cdot scal}$[b] (cm^{-1})	int.	freq.$_{\cdot scal}$[b] (cm^{-1})	int.	freq.$_{\cdot scal}$[b] (cm^{-1})	int.	freq.$_{\cdot scal}$[b] (cm^{-1})	int.	freq.$_{\cdot scal}$[b] (cm^{-1})	int.	freq.$_{\cdot scal}$[b] (cm^{-1})	int.	freq.$_{\cdot scal}$[b] (cm^{-1})	int.	freq.$_{\cdot scal}$[b] (cm^{-1})	int.	freq. (cm^{-1})	int.[c]
γCOO									713.4	15							708.7	14	732; 727;	sh; sh;
$\delta C_\alpha C_\beta O$													693.3	20					721	m
δC-O$_C$																	643.3	5		
δC=O	640.6	17																	645	m
δC-O$_C$									638.4	11										
δC=O											627.0	49							633	w
τC-O$_C$							625.0	80											617	m
δC=O							588.6	121							598.1	22			587	m
τC-O$_C$													593.8	120					579	m
τC-O$_A$					589.9	64														
τC-O$_C$											585.6	117								
$\delta C_\alpha C_\beta O$			584.3	6															568	s
τC-O$_C$	582.4	111																		
δC-O$_C$					571.4	75														
τC-O$_A$	554.4	133					556.1	55											566	s
δC=O									548.6	9							550.9	7		
δC=O													562.2	129					561	m
τC-O$_A$											546.0	95							546	vw
$\nu C_\alpha C$			537.2	7															531	sh
δC=O					533.5	5													526	sh
δCC(C)N											528.7	42								
$\rho C_\beta C_\alpha C$							515.9	27											521;	m;
τC-O$_A$													515.5	79						
δC-O$_C$	514.4	9													514.5	1			518	m
δC-O$_C$			506.9	3																
δC-O$_C$							470.6	33											494	m
$\delta C_\alpha C_\beta O$																	420.2	22		
$\delta NC_\alpha C$									413.1	7					416.0	10				
$\delta C_\alpha C_\beta O$					407.3	3														
$\delta NC_\alpha C$											401.5	14								
τC-O$_A$			399.7	93															408	w
$\delta NC_\alpha C$	397.8	28																		
δC-O$_C$													371.2	6						
δCC(C)N															362.5	12				
$\delta NC_\alpha C$			359.3	20			357.7	3												

[a] See Table S3 for definition of coordinates. [b] The scale factor used for all modes was 0.978, except for the two $\nu OH_{A/C}$. The scale factor used for νOH_A in all conformers and for νOH_C in **A** and **C** conformers was 0.953; the factor 0.913 was used to scale νOH_C modes of **B** conformers (see Experimental section for details). [c] Experimental IR intensities are presented in a qualitative way (vw, very weak; w, weak; m, medium; s, strong; vs, very strong; sh, shoulder; vb, very broad). For the lowest intensity bands predicted by calculations lying at nearly the same frequency of more intense bands, the assignments were made as an indication that these bands should also contribute to the experimental bands as a minor species.

occurring preferentially for those conformers where the carboxylic group is not engaged in H-bond as proton donor. The reason for the observed specific preference for the **C** conformer relative to the **A** conformers can be related with the presence in the **C** conformer of the stronger O−H$_A$···O= bond instead of the considerably weaker N−H···O= bond present in the **A** conformers. The different rates of decarboxylation associated with the three groups of serine conformers strongly facilitated the assignment of the experimental spectra. This is clearly demonstrated in the case of the νO−H stretching spectral region in Figure 4, but it does also apply to the other regions of the spectra, as will be stressed further below.

(iv) Besides aggregation, which can be noticed by appearance of characteristic bands of aggregates throughout the spectra, annealing of the matrixes led only to minor spectral changes, from which the most relevant is the increase of the intensity of the bands with predominant contribution from conformers **1** and **3** relative to bands due to other conformers. This is illustrated in Figure 4 by the relative increase of intensity of the bands at 3567 and 3556 cm^{-1}, due to conformer **1** and at 3543 cm^{-1}, ascribed to conformer **3**. When annealing of the matrix is done, conversion from the less stable conformers into an energetically accessible lower energy form shall take place. The energy barriers separating the reactant conformers from the products shall be low enough to be overcome at the low work temperature. As a rough estimate of the barriers of interconversion between the different experimentally observed conformers of serine in the low-temperature matrixes, the DFT/B3LYP/6-311++G(d,p) barriers for the molecule in a vacuum were calculated (see Table S22 of the Supporting Information; the COOH cis ↔ COOH trans interconversion is well-known to have associated barriers of more than ca. 40 kJ mol^{-1} [58] and was not here subjected to calculation). The calculated barriers are, in general, predicted to be relatively high. Indeed, in many cases, the simultaneous rearrangement of several groups, as well as breaking of H bonds, are required for the molecular system to undergo a transition from one conformer to other of lower energy. However, taking into account the margin of error associated with the unavoidable intrinsic errors in the theoretical estimations as well as the effects of the environment, the calculated values for the energy barriers are compatible with observation of, at least, some conformational rearrangements upon annealing of the matrixes. If we took into consideration the theoretical results just as an indicator of the relative accessibility of the various processes (by looking at the relative values of the barriers), then, in consonance with the experimental observations, for cis carboxylic conformers (**A** and **C** conformers), one could expect an increase of population of conformer **1**, particularly at expenses of both forms **4** and **7** (conformer **6** might also be converted to **1** in a two step process **6** → **4** →**1**; see Table S22). In the case of trans carboxylic conformers (**B** conformers), the theoretically predicted energy barriers are consistent with conversion from conformers **5**, **8**, and **9** either in conformer **2** or/and **3** (energy barriers leading to production

TABLE 4: Calculated DFT/B3LYP/6-311++G(d,p) for the Nine Most Stable Conformers of D,L-3,3-Dideutero-serine and Experimental MI-IR Spectrum (Argon)

	1		2		3		4		5		6		7		8		9		exptl	
approx. descript.[a]	freq.scal[b] (cm^{-1})	int.	freq.scal[b] (cm^{-1})	int.	freq.scal[b] (cm^{-1})	int.	freq.scal[b] (cm^{-1})	int.	freq.scal[b] (cm^{-1})	int.	freq.scal[b] (cm^{-1})	int.	freq.scal[b] (cm^{-1})	int.	freq.scal[b] (cm^{-1})	int.	freq.scal[b] (cm^{-1})	int.	freq. (cm^{-1})	int.[c]
νOH_A															3669.8	48			3664	w
νOH_A									3667.6	52									3660	w
νOH_A																	3651.1	42	3637	w
νOH_A			3640.3	48															3630; 3629	w
νOH_A													3601.8	66					3610	w
νOH_C							3585.9	83											3594	w
νOH_C											3579.9	79							3589	sh
νOH_C	3573.8	68																	3567	m
νOH_C													3570.4	74					3564	m
νOH_A							3552.3	62			3555.6	70							3560	m
νOH_A	3551.3	73																	3556; 3551	s; sh
νOH_A					3545.0	137													3543	sh
νNH_2 as.	3505.6	13	3509.7	16	3513.8	13	3527.9	23	3498.0	22	3515.4	12	3517.6	13	3507.8	12	3499.1	21	3518	sh
νNH_2 s.							3439.7	13			3437.9	5							3427	w
νNH_2 s.					3428.1	24			3431.4	2			3430.0	4			3429.9	4	3418	w
νNH_2 s.	3425.4	7													3425.0	7			3413	w
νNH_2 s.			3418.0	16															3404	w
νOH_C			3163.3	276	3184.3	236			3155.5	292					3174.8	274	3168.4	274	≈3175	vb
$\nu C_\alpha H$	3004.9	7	2972.6	10	2982.7	5	2916.7	30	2976.8	14	3018.9	6	2971.7	17	2977.9	6	2954.3	25	2974; 2962; 2897; 2883	vw; sh; sh; vw
νCD_2 as.	2247.8	12	2254.2	12			2253.2	11			2245.8	12	2251.8	12			2256.5	8	2238; 2231; 2225; 2217; 2213; 2204	w; sh; sh; vw; vw; vw
νCD_2 as.					2222.8	20			2230.4	12					2227.4	13			2183	w
νCD_2 s.			2167.9	21													2168.1	13	2126	w
νCD_2 s.	2121.0	33			2113.6	37	2130.3	42	2135.0	23	2121.1	33	2151.4	29	2127.1	29			2111; 2108; 2099	w; w; sh
$\nu C{=}O$									1795.1	352					1792.3	338	1793.4	348	1787; 1785	s; s
$\nu C{=}O$			1785.2	328															1778	sh
$\nu C{=}O$	1766.3	315			1771.0	308													1773	vs
$\nu C{=}O$	1766.3	315					1769.4	306			1769.5	317							1771	vs
$\nu C{=}O$													1744.2	305					1753; 1752	s; sh
δNH_2	1633.0	35	1616.4	38	1622.6	37	1600.9	71	1631.1	38	1628.4	38	1609.3	40	1631.2	37	1630.4	38	1646; 1600; 1560; 1527	w; w; w; w
$\rho C_\beta C_\alpha H$	1392.4	5																	1401	m
δCOH_C			1384.8	412	1381.6	299			1387.1	382					1384.7	402	1382.4	381	1385; 1380	s; sh
$\rho C_\beta C_\alpha H$							1378.1	22			1376.1	12			1374.0	13			1372	s
ρNH_2													1362.7	14					1358;	m;
$\rho C_\beta C_\alpha H$			1356.6	3	1356.3	37													1355	sh
$\rho C_\beta C_\alpha H$													1350.3	33					1343;	sh;
δCOH_A					1349.1	205														
$\delta C_\beta C_\alpha H$									1340.5	23									1338	sh
$\delta C_\beta C_\alpha H$																	1330.1	21	1333;	m;
δCOH_A	1332.8	83					1326.5	74			1328.0	99							1323	m
δCOH_A													1312.4	53						
δCOH_C; $\nu C\text{-}O_C$											1309.5	58								
δCOH_C	1304.6	73																	1306;	w;
δCOH_C							1296.1	23											1290;	w;
δCOH_A															1292.1	8			1278;	w;
$\rho C_\beta C_\alpha H$									1291.0	5							1291.7	13	1270;	w;
δCOH_A			1283.2	36					1281.5	7									1264	m
$\delta C_\beta C_\alpha H$							1272.5	30												
δCOH_A																	1269.1	41		
δCOH_C													1267.1	9						
$\delta C_\beta C_\alpha H$			1255.1	18	1260.8	2					1260.4	2			1263.2	9			1239	w
$\delta C_\beta C_\alpha H$	1236.9	11																	1220	w
ρNH_2									1217.3	4										
$\nu C\text{-}O_C$																	1212.0	14	1209;	w;
ρNH_2	1208.9	14																	1204;	w;
ρNH_2							1200.6	31			1203.2	17							1196;	w;
$\delta C_\beta C_\alpha H$													1196.5	26					1189	w;
$\nu C\text{-}O_C$			1182.6	24	1193.0	18									1182.7	19			1186	w
ρNH_2			1177.8	17	1174.7	14									1179.6	3				
$\nu C\text{-}O_C$									1162.0	31									1161;	m;
ρNH_2																	1157.8	20	1157	m
$\nu C_\alpha C_\beta$			1147.6	41									1146.6	82					1151; 1149	m; m

TABLE 4 (Continued)

	1		2		3		4		5		6		7		8		9		exptl	
approx. descript.[a]	freq.-scal[b] (cm^{-1})	int.	freq.-scal[b] (cm^{-1})	int.	freq.-scal[b] (cm^{-1})	int.	freq.-scal[b] (cm^{-1})	int.	freq.-scal[b] (cm^{-1})	int.	freq.-scal[b] (cm^{-1})	int.	freq.-scal[b] (cm^{-1})	int.	freq.-scal[b] (cm^{-1})	int.	freq.-scal[b] (cm^{-1})	int.	freq. (cm^{-1})	int.[c]
νC-O$_C$	1140.3	76																		
νC-O$_C$; δCOH$_C$											1138.7	245							1137	s
νC-O$_C$							1137.5	145											1134	s
νC-O$_A$							1131.3	68											1132	sh
νC-O$_A$	1125.5	49			1126.6	13					1123.6	34							1131	sh
νC-O$_C$													1121.7	241					1124	m
ωCD$_2$																	1114.0	85	1109;	vs;
νC-O$_A$															1113.9	11			1108;	sh;
νN-C											1108.7	8							1105;	s;
δCD$_2$					1102.5	47			1110.2	12									1103	sh
νN-C	1096.3	195															1100.0	11		
δCD$_2$															1087.1	18			1099;	sh;
																			1097;	m;
νN-C							1080.4	71	1078.3	36									1090;	sh;
νC$_\alpha$C$_\beta$															1077.7	91			1087;	m;
δCD$_2$	1076.0	2	1075.6	3			1082.5	6			1072.4	1	1078.5	5					1086	m;
νN-C			1072.6	14																
δCD$_2$																	1068.6	1		
νN-C					1063.3	15													1069	w
ωCD$_2$									1061.6	87										
νN-C													1054.7	2					1049	w
νC$_\alpha$C$_\beta$					1001.2	66													1015;	w;
																			1013	sh
ωNH$_2$															989.8	128			1004;	sh;
																			993;	m;
ωCD$_2$	984.4	54									980.2	61							987	sh
ωCD$_2$							971.0	31					970.7	27					981;	sh;
																			979;	sh;
ωNH$_2$									966.6	123							965.5	111	977;	sh;
ωCD$_2$			965.9	47	964.8	8													975	m
νC-O$_A$													959.4	32			959.0	30	971	m
νC-O$_A$			951.8	57					951.5	8									969;	m;
ωCD$_2$															944.3	6			968	m
νC$_\alpha$C	937.9	26																	962;	m;
																			960;	sh;
																			957	m
νC$_\alpha$C$_\beta$											922.3	21							947;	w;
νC$_\alpha$C							916.8	14											946;	sh;
νC$_\alpha$C$_\beta$									912.8	34									944	w
twCD$_2$					910.0	<1														
νC$_\alpha$C$_\beta$	901.8	32															903.8	41	934;	sh;
																			930;	w;
twCD$_2$									899.9	3									928;	w;
twCD$_2$															895.0	25			921	sh
ωNH$_2$											889.9	55							912;	w;
ρCD$_2$															887.6	41			909;	sh;
twCD$_2$	882.4	29	883.7	47			883.2	62			881.6	47	878.0	32					906;	vw;
ρCD$_2$					879.3	38													905	vw
twCD$_2$																	870.6	9	890;	sh;
ωNH$_2$			866.2	88			861.5	44											889	s
τC-O$_C$									856.3	68									880	w
νC$_\alpha$C															850.2	29			856;	m;
																			853;	sh;
τC-O$_C$			848.1	70	849.9	81											847.1	68	847	sh
νC$_\alpha$C									842.2	39							837.4	51	834	sh
τC-O$_C$															836.7	99				
ωNH$_2$													831.9	88					824	s
ωNH$_2$	831.2	131																	823	s
ωNH$_2$					820.3	123													817;	sh;
νC$_\alpha$C$_\beta$							820.3	61											814;	m;
νC$_\alpha$C											811.2	103							813	m
γCOO			798.2	25									797.7	33					805;	sh;
																			802;	m;
																			799;	w;
																			795;	sh;
																			789	vw
ρCD$_2$													779.3	50					776	m
ρCD$_2$	764.6	13							761.6	17	762.5	23							774;	m;
																			772;	m;
νN-C															760.6	6			771;	sh;
																			767	m
ρCD$_2$			756.4	2			758.4	26									755.7	20	760;	m;
																			757;	w;
																			756	sh
νC$_\alpha$C; δC=O					749.2	6													753	sh
δC=O			738.8	11															750;	sh;
																			749	m
							718.6	30											730;	m;
δC=O													719.5	34					727	sh

TABLE 4 (Continued)

	1		2		3		4		5		6		7		8		9		exptl	
approx. descript.[a]	freq.scal[b] (cm^{-1})	int.	freq.scal[b] (cm^{-1})	int.	freq.scal[b] (cm^{-1})	int.	freq.scal[b] (cm^{-1})	int.	freq.scal[b] (cm^{-1})	int.	freq.scal[b] (cm^{-1})	int.	freq.scal[b] (cm^{-1})	int.	freq.scal[b] (cm^{-1})	int.	freq.scal[b] (cm^{-1})	int.	freq. (cm^{-1})	int.[c]
γCOO											714.8	30							720;	vw;
δC=O															712.7	12			716	sh
γCOO	708.1	33																	710	m
γCOO									702.6	14										
γCOO																	697.6	13	695;	w;
γCOO					685.7	17													691	sh
$\delta C_\alpha C_\beta O$													676.5	18						
δC-O$_C$																	638.9	4		
δC=O	638.5	17																	641	w
δC-O$_C$									633.6	11										
δC=O											625.8	47							631	m
τC-O$_C$							622.3	81											613	m
τC-O$_C$													590.9	115					583; 581; 577	m
γCOO															589.8	19			567;	sh;
$\tau C_\beta O$					585.9	80													565	sh
τC-O$_C$											579.8	100								
τC-O$_A$							577.5	157											563	s
τC-O$_C$	576.0	85																		
δC-O$_C$					567.5	55													560;	s;
$\delta C_\alpha C_\beta O$			563.1	5															558;	sh;
τC-O$_A$	553.3	152																	554;	w;
δC=O							547.7	16											551	vw
τC-O$_A$											541.1	144	545.7	163					540	m
δC=O									531.1	6							530.3	3	531	w
$\nu C_\alpha C$			530.5	7																
$\nu C_\alpha C$;					523.3	4													525;	w;
δC=O																			524;	w;
																			521	sh
δC-O$_C$											510.6	5							508;	m;
$\nu C_\alpha C$													508.7	42					506;	m;
γCOO							506.5	26											505;	m;
δC-O$_C$															506.9	1			503	m
δC-O$_C$	493.5	10	495.9	2															491	w
δC-O$_C$							465.4	30											477	m
$\delta C_\alpha C_\beta O$					401.7	3			397.7	10							404.3	23		
τC-O$_A$			397.1	102															402	w
$\delta C_\alpha C_\beta O$															392.7	13				
$\delta NC_\alpha C$	390.3	24									391.6	12								

[a] See Table S3 for definition of coordinates. [b] The scale factor used for all modes was 0.978, except for the two nOHA/C. The scale factor used for nOHA in all conformers and for nOHC in **A** and **C** conformers was 0.953; the factor 0.913 was used to scale nOHC modes of **B** conformers (see the Experimental Section for details). [c] Experimental IR intensities are presented in a qualitative way (vw, very weak; w, weak; m, medium; s, strong; vs, very strong; sh, shoulder; vb, very broad). For the lowest intensity bands predicted by calculations lying at nearly the same frequency of more intense bands, the assignments were made as an indication that these bands should also contribute to the experimental bands as a minor species.

of **2** and **3** from **5**, **8**, and **9** are of the same order of magnitude). However, accordingly with the experimental observations, pathways leading to production of conformer **3** appear to be favored.

A final note shall be made regarding the assignments now proposed for the νOH and νNH_2 stretching region (3700−3100 cm^{-1}) in comparison with those previously made by Lambie et al.,[29] which in some cases differ considerably from ours. The present assignments are supported by a complete theoretical analysis of the conformational space of the molecule and calculation of the IR spectra of all relevant conformers, which indeed were found to be nine instead of the four previously considered. The assignments were also supported by the irradiation and annealing experiments, which promoted changes in the relative populations of the conformers, facilitating identification of the bands due to individual conformers. Finally, use of deuterated species provides additional data for further validation of the assignments now presented. As it will be shown in the next sections, the same can be stated for the interpretation of the other spectral regions.

νC_β(H/D)$_2$ and νC_αH Stretching Regions (3100−2800 and 2260−2000 cm^{-1}). The νC_α-H/D vibrations have been recently shown to provide information about the involvement of a hydroxyl group attached in the α position in hydrogen bonding interactions.[59] For the model compound *n*-[1-D]propanol, the νC_α-H/D frequency could be successfully correlated with the H-bond strength in a series of different experimental conditions, which included the matrix isolated compound (argon), pure liquid and low temperature glassy states, and solution in different solvents. However, it was found that such correlation can only be established when the OH group is not acting simultaneously as proton donor and acceptor.[59] In serine conformers, with a few exceptions (see Figure 1), this last condition is not fulfilled. Hence, it is not expected that the analysis of this spectral region could provide any information that can be considered particularly significant regarding H-bonding in the studied compound. Nevertheless, some useful information could still be extracted from an analysis.

First, upon UV irradiation of the matrixes, intensity changes in the complex profiles of the νCH/D stretching bands were found to be consistent with the appearance of new bands at frequencies expected for νCH/D stretching vibrations in ethanolamine. In the case of the nondeuterated compound, an increase of intensity was noticed at ca. 2866 cm^{-1}, that is at a frequency similar to those corresponding to the ethanolamine νCH_2 symmetric stretching modes (2882 and 2861 cm^{-1}).[60,61] The bands due to antisymmetric vibrations have been observed previously at ca. 2950 cm^{-1},[60,61] but could not be detected in

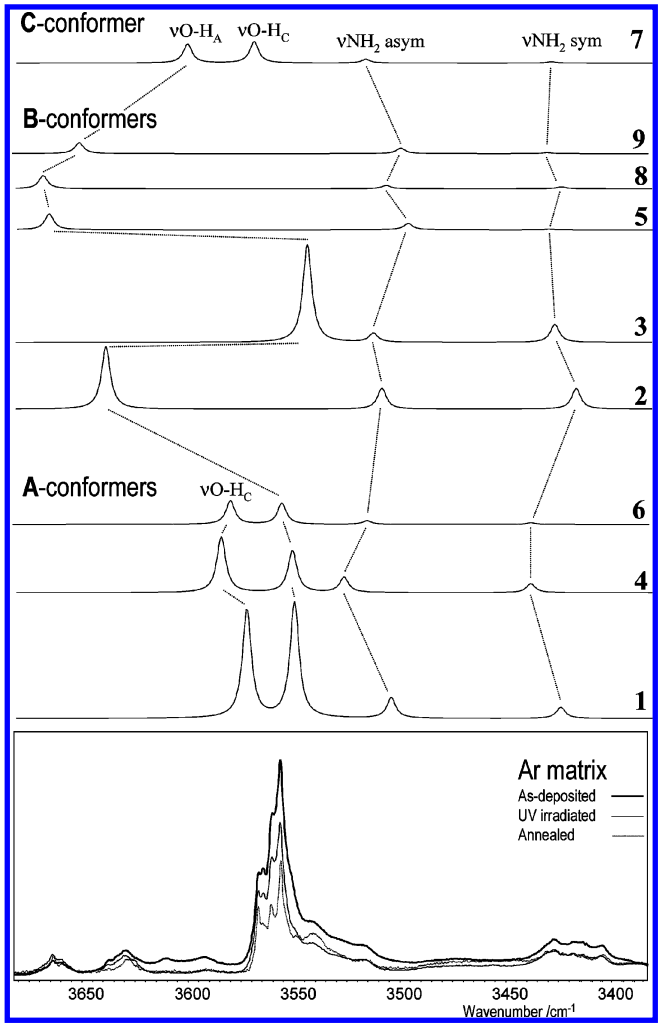

Figure 4. νO−H and νNH_2 stretching region (above 3350 cm^{-1}) of the IR spectrum of matrix-isolated serine (Ar matrix) and spectra calculated at the DFT/B3LYP/6-311++G(d,p) level (wavenumbers were scaled: positions of the bands due to νNH_2 by a factor of 0.978, of the bands due to νOH in the spectra of forms **1**, **3**, **4**, and **6** by a factor of 0.913, and of the bands due to νOH in the spectra of forms **2**, **5**, **7**, **8**, and **9** by a factor of 0.953) for the nine experimentally relevant conformers. In the calculated spectra, intensities are multiplied by the estimated relative populations. As mentioned in the text, $\nu O-H_C$ of the H-bonded B-type conformers are observed as a broad band centered around 3170 cm^{-1}.

the present study since they fall in a more congested spectral region. However, in the spectrum of 3,3-dideutero-serine, the four bands expected for the photoproduced deuterated ethanolamine (symmetric and antisymmetric νCH_2 and νCD_2 stretching modes) can be assigned to the bands emerging at 2950−2903, 2870, 2214, and 2100 cm^{-1}. As expected, the νCH_2 bands were then observed at similar frequencies in both deuterated and nondeuterated molecules, whereas the νCD_2 bands were observed at frequencies closely matching those predicted by the DFT(B3LYP)/6-311++G(d,p) calculations: 2223 and 2112 cm^{-1}. Hence, these observations strongly support the idea that ethanolamine, together with CO_2, is the major photoproduced species.

An additional band appearing in this region upon UV irradiation is observed at 2276 cm^{-1}. The origin of this band is uncertain, but it might be tentatively assigned to methyl isocyanate (CH_3NCO), which can result from photolysis of acetamide (CH_3NCO would be formed together with H_2). Note that CH_3NCO should also absorb around 776 cm^{-1}, and in fact,

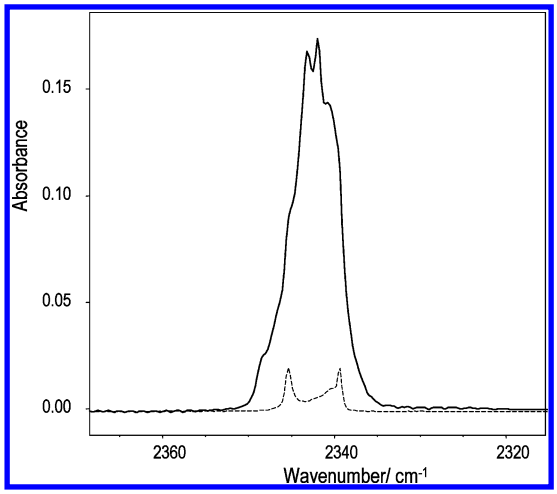

Figure 5. CO_2 asymmetric stretching spectral region of the serine irradiated matrix (solid line) and of free CO_2 isolated in argon (dashed line).

the spectral intensity in the 780−765 cm^{-1} region increases after irradiation, thus supporting the assignment of the 2276 cm^{-1} band to CH_3NCO.

Finally, the annealing experiments reveal that the low-frequency region of the feature assigned to the νCH_2 symmetric stretching vibration increases in intensity relative to all other features observed in the 3100−2800 cm^{-1} spectral range. Very interestingly, the calculations predicted that the conformers of serine where νCH_2 symmetric stretching should occur at lowest frequency were conformers **1** and **3** (see Table 3). Hence, the analysis of this spectral region is also consistent with an increase of population of these two conformers upon annealing of the matrix, reinforcing the conclusions extracted from the analysis of the νOH stretching region.

νC═O Stretching Region (1850−1700 cm^{-1}). In this spectral region, the spectra of both isotopologues of serine are very similar to each other. Six main bands due to monomeric serine are observed between 1850 and 1740 cm^{-1} (Figure 6). The absorptions with maximum at ca. 1720 cm^{-1}, that increased considerably upon annealing are originated in aggregates, appearing at similar frequencies observed for aggregates of analogous compounds.[62] According to the calculations, **B** conformers should give rise to νC═O bands appearing at higher frequencies than **A** conformers, whereas conformer **7** (of the **C**-type) should absorb at a considerably lower frequency than all of the other forms (see Figure 6). Conformer **3** (**B**-type) is once again an exception to the regularities found for other **B**-type conformers. The reason for that could be the presence in this form of the relatively stronger OH_A···O═ H bond that reduces the frequency of the carbonyl stretching mode and makes the experimental frequency of the νC═O band in **C** similar to the corresponding values in **A** group of conformers.

In consonance with the theoretical predictions, the νC═O modes of conformers **5**, **8**, and **9** are assigned to the two overlapping higher frequency bands observed in this region at 1790 and 1788 cm^{-1}, whereas conformer **2** gives rise to the band at 1778 cm^{-1}. In conformers **5**, **8**, and **9**, the carbonyl group is not participating in any H bond. The two intense bands at 1773 and 1771 cm^{-1} are due to **A**-type conformers and conformer **3**. Upon irradiation of the matrix, the band at 1771 cm^{-1} decreases considerably in intensity, whereas the band at 1773 cm^{-1} does not change very much. This result indicates that the lowest-frequency band is essentially due to **A**-type conformers, whereas conformer **3** shall contribute to the highest frequency band. On the other hand, upon annealing (after

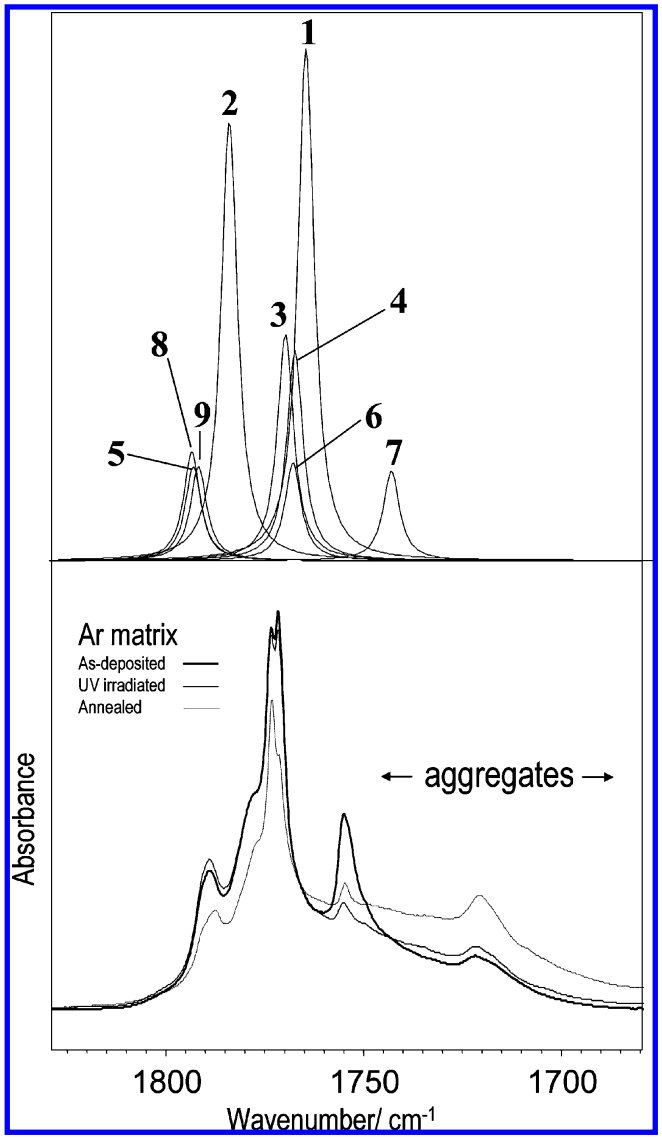

Figure 6. Carbonyl stretching region of the IR spectrum of matrix-isolated serine (Ar matrix) and Simulated DFT/B3LYP/6-311++G-(d,p) spectra (scaled; see Materials and Methods section for details) for the nine experimentally relevant conformers. In the calculated spectra, intensities are multiplied by the estimated relative populations.

irradiation), the band at 1771 cm^{-1} decreases in intensity, whereas the 1773 cm^{-1} band increases. Since bands due to conformers **1** and **3** are expected to increase in intensity upon annealing and those due to other conformers are expected to decrease, the results of the annealing experiments seem to indicate that conformer **1** shall also contribute to the 1773 cm^{-1} band. Thus, on the whole, the experimental results indicate that conformer **1** shall contribute to both the 1773 and 1771 cm^{-1} bands, whereas conformer **3** and other **A** conformers (forms **4** and **6**) should contribute only to the high-frequency and low-frequency bands, respectively.

The calculations predict also that the lowest-frequency νC=O band ascribable to monomeric serine (1755 cm^{-1}; with a shoulder at lower frequency in the case of the deuterated compound) is due to the **C**-type conformer **7**. This assignment is unequivocal, in particular due to the behavior exhibited by this band upon UV irradiation: as expected, it is, among all bands in this spectral region, the one showing a larger intensity reduction (see Figure 6).

δCOH Bending Region (1420−1200 cm^{-1}). The δCOH vibrations in the different serine conformers are predicted by the calculations to give rise to IR bands appearing in a relatively broad spectral range extending over ca. 220 cm^{-1} (see Tables 3 and 4 and also S4−S21). The frequencies of the δCOH vibrations obey the general rule that the stronger a H-bond is, the higher the frequency of the δCOH vibration should be. This rule should be valid for both alcohol and carboxylic OH groups. The δCOH_C modes in the **A** and **C** conformers (which have their OH_C group "free") are predicted by the calculations to give rise to low-intensity IR bands (5−50 km mol^{-1}) in the 1310−1274 cm^{-1} region, whereas for the H-bonded **B** conformers, the δCOH vibrations shall give rise to intense (220−470 km mol^{-1}) bands at 1400−1375 cm^{-1}. On the other hand, δCOH_A bands are predicted to have significantly lower intensities (<70 km mol^{-1}). For all **B** conformers with a "free" OH_A group, the IR bands due to δCOH_A vibrations are predicted to appear in the 1205−1211 cm^{-1} region. Conformers **A** and **C**, with relatively weak H bonds involving the alcohol group as a proton donor, are expected to absorb within the 1340−1400 cm^{-1} spectral region. Finally, for conformer **3**, with a stronger OH_A···O= H bond, the δCOH_A band is predicted to appear at the highest frequency around 1420 cm^{-1}. In summary, for conformers **A** and **C** (plus conformer **3**), the frequencies of the δCOH_A vibrations are predicted to be higher than the frequencies of the δCOH_C vibrations, whereas for the **B** conformers (except for **3**) the reversed order of frequencies is expected.

Since in this spectral region the bands not only due to δCOH modes, but also due to other vibrations (e.g., C−H deformations) do also appear, the complexity of the spectra precludes a detailed assignment to the bands observed in the experimental spectra to the different conformers. However, the general pattern extracted from the analysis of the theoretical spectra reflects well in the experimental data. Figure 7 displays the region between 1460 and 1350 cm^{-1} of the spectrum of serine and compares the experimental data with a schematic representation of the calculated spectra for the conformers absorbing in this spectral region. In this figure, only the calculated bands ascribed to δCOH modes are represented for simplification (the most intense bands due to other vibrations appearing in this region are explicitly indicated in the experimental spectra and refer to the twisting and wagging modes of conformer **2** as well as to the band here assigned to $\delta C_\beta H_2$ in conformers **2**, **7**, and **9**; see also Table 3). The intense bands due to the δCOH_C vibrations of **B** conformers can be easily identified. Following the general pattern already mentioned, these bands are only slightly affected by UV irradiation. In addition, for all **B** conformers but conformer **3**, the bands substantially decrease in intensity upon annealing. In the case of the δCOH_C band of conformer **3**, at ca. 1376 cm^{-1}, the apparent decrease of intensity upon annealing results from loss of intensity of the deformation bands originated in conformer **2** (and also the δCOH_C bands of conformers **5**, **8**, and **9**, assigned to the feature around 1384 cm^{-1}) that extensively overlap with this band. However, it is clear that the 1376 cm^{-1} band gains in relative intensity compared with the neighboring bands. As expected, the δCOH_A band due to **A** and **C** conformers (mainly conformer **1**), observed as a shoulder at 1410 cm^{-1}, slightly increases upon annealing. With all probability, the δCOH_A band of conformer **3** is also contributing to the total intensity of the shoulder due to **A** and **C** conformers. The broad band emerging at frequencies between 1450 and 1420 cm^{-1} upon annealing is due to aggregated forms, where the hydroxyl groups can be expected to participate in considerably strong intermolecular H bonds, hence, giving rise to δCOH modes absorbing at high frequencies.

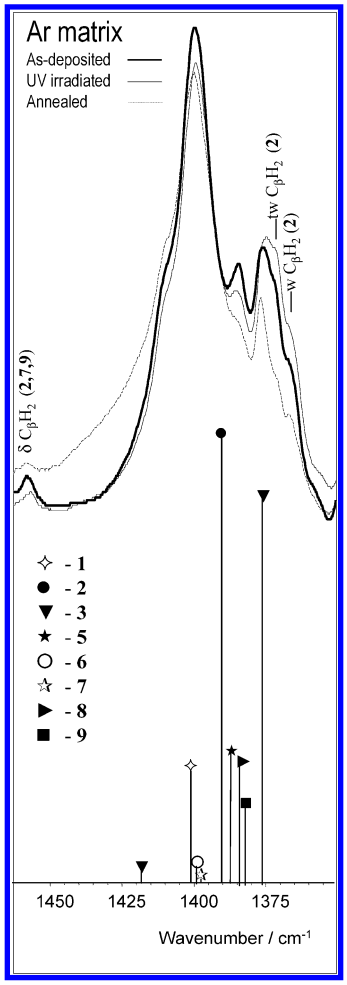

Figure 7. δCOH bending spectral region of D,L-serine in argon matrix and Simulated DFT/B3LYP/6-311++G(d,p) spectra (scaled; see Materials and Methods section for details) for the nine experimentally relevant conformers in the 1460−1350 cm^{-1} spectral region. In the calculated spectra, intensities are multiplied by the estimated relative populations. In the figure, only the calculated bands ascribed to δCOH modes are represented for simplification (the most intense bands due to other vibrations appearing in this region are explicitly indicated in the experimental spectra and refer to the twisting and wagging modes of conformer **2** as well as to the band here assigned to $\delta C_\beta H_2$ in conformers **2**, **7**, and **9**; see also Table 3).

The IR bands observed in the region 1350−1200 cm^{-1} are characterized by a relative low intensity. In this spectral range, band overlap is extensive, hindering the assignment of the bands due to δCOH modes originated in "free" OH groups. Interestingly, in this region, UV irradiation leads to emergence of a band around 1230 cm^{-1} that appears at nearly the same frequency of one of the twCH2 vibrations of ethanolamine.[57] Note that ethanolamine has also two bands at 1385 and 1375 cm^{-1} (ωCH_2[57]), which are probably very responsible for the small increase of intensity of the bands at nearly these frequencies ascribed to the twisting and wagging modes of conformer **2** of serine upon irradiation (see Figure 7).

νC−O and νN−C Stretching Region (1200 − 950 cm^{-1}). The νC−O ($\nu C-O_C$ and $\nu C-O_A$) and νN−C stretching modes are predicted by the calculations to give rise to bands in the 1200−950 cm^{-1} region. Both $\nu C-O_C$ and νN−C frequencies were shown not to be greatly affected by deuteration at the C_β atom, and the expected pattern of variation with conformation was found to be identical in the two isotopologues studied. On the other hand, $\nu C-O_A$ vibration was predicted to be strongly affected by deuteration, since in the deuterated compound it was found to couple extensively with the ωCD_2 wagging oscillation (see Tables S13−S21). For each conformer of serine, besides νC−O and νN−C stretching modes many other vibrations were predicted to give rise to bands in the 1200−950 cm^{-1} spectral range. However, calculations also indicated that most of those vibrations should give rise to bands of low relative intensity.

In **B** conformers, $\nu C-O_C$ is expected to originate low-intensity bands (<30 km mol^{-1}) at frequencies between 1200 and 1160 cm^{-1}, whereas in both **A** and **C** conformers, this vibration shall give rise to more intense bands (76−320 km mol^{-1}) appearing at lower frequencies (1135−1120 cm^{-1}). Hence, these results indicate that in the studied compounds the $C-O_C$ bond is weaker for a cis carboxylic group (as in **A** and **C** conformers) than in a trans carboxylic group (as in the **B** conformers), correlating well with the structural data presented above, which indicate that the $C-O_C$ bond is longer in **A** and **C** conformers than in **B** forms (see also Table S2).

In various conformers, the $\nu C-O_A$ and νN−C vibrations are coupled with oscillations along other coordinates. Hence, for the normal modes involving the $\nu C-O_A$ and νN−C vibrations, it is difficult to extract a clear pattern of variations introduced by changes in conformational structure (see Tables S3−S21). Nevertheless, it can still be stated that in general $\nu C-O_A$ shall correspond to a relatively intense band (ca. 100 km mol^{-1} for all but the **C** conformer) appearing for nondeuterated serine between 1060 and 960 cm^{-1}. In all conformers of deuterated serine, extensive mixing with the ωCD_2 wagging coordinate shall lead to the appearance of two bands with low intensity, at ca. 950 and 1130 cm^{-1}, with substantial contribution from both $\nu C-O_A$ and ωCD_2 modes. On the other hand, νN−C is in general predicted to give rise to a weak band at ca. 1060−1100 cm^{-1} (a few exceptions can be noticed, concerning, for instance, conformers **1** and **4** in both deuterated and nondeuterated species and conformer **2** in the nondeuterated compound, where this mode is predicted to correspond to a relatively intense IR band).

In this spectral region, the experimental spectrum of the nondeuterated compound is dominated by bands due to the most stable conformer **1** at ca. 1150 ($twCH_2$), 1137 ($\nu C-O_C$), 1105 (νN−C), and 1065 ($\nu C-O_A$) cm^{-1}. In consonance with the calculations, all of these bands should also overlap (or partially overlap) with bands due to other conformers, justifying the observations of a less clear pattern of variation upon irradiation and annealing. The remaining seven intense bands in this spectral region (at 1168, 1163, 1132, 1126, 1123, 1057, and ca. 975 cm^{-1}) belong to the spectra of conformers other than the form **1**. The 1168 cm^{-1} band is ascribable to both conformers **6** ($twCH_2$) and **8** (ρNH_2), the 1163 cm^{-1} band to conformer **5** ($\nu C-O_C$), 1132 cm^{-1} to **4** ($\nu C-O_C$), 1126 cm^{-1} to **6** ($\nu C-O_C$), 1123 cm^{-1} to **7** ($\nu C-O_C$), 1057 cm^{-1} to both **2** (γCH_2) and **4** ($\nu C-O_A$), and, finally, 975 cm^{-1} to **2** ($\nu C-O_A$). The assignment of the band observed at 1123 cm^{-1} to the most intense band predicted by the calculations for conformer **7** is particularly unambiguous, since upon irradiation this band practically disappears. As expected, all bands due to $\nu C-O_C$ of **A** and **C** conformers (predicted to be intense) are clearly observed, whereas for **B** conformers, only the band due to conformer **5** could be experimentally identified. The relatively intense $\nu C-O_A$ bands in **A** and **B** conformers were also observed (**1**, **3**, and **6**, 1065 cm^{-1}; **4**, 1057 cm^{-1}; **5** and **9**, 1043 cm^{-1}; **8**, 1010 cm^{-1}; and **2**, 975 cm^{-1}).

The analysis of the spectrum of deuterated serine, which in this region is somewhat less complex than that of nondeuterated serine, reinforced the general conclusions extracted from the

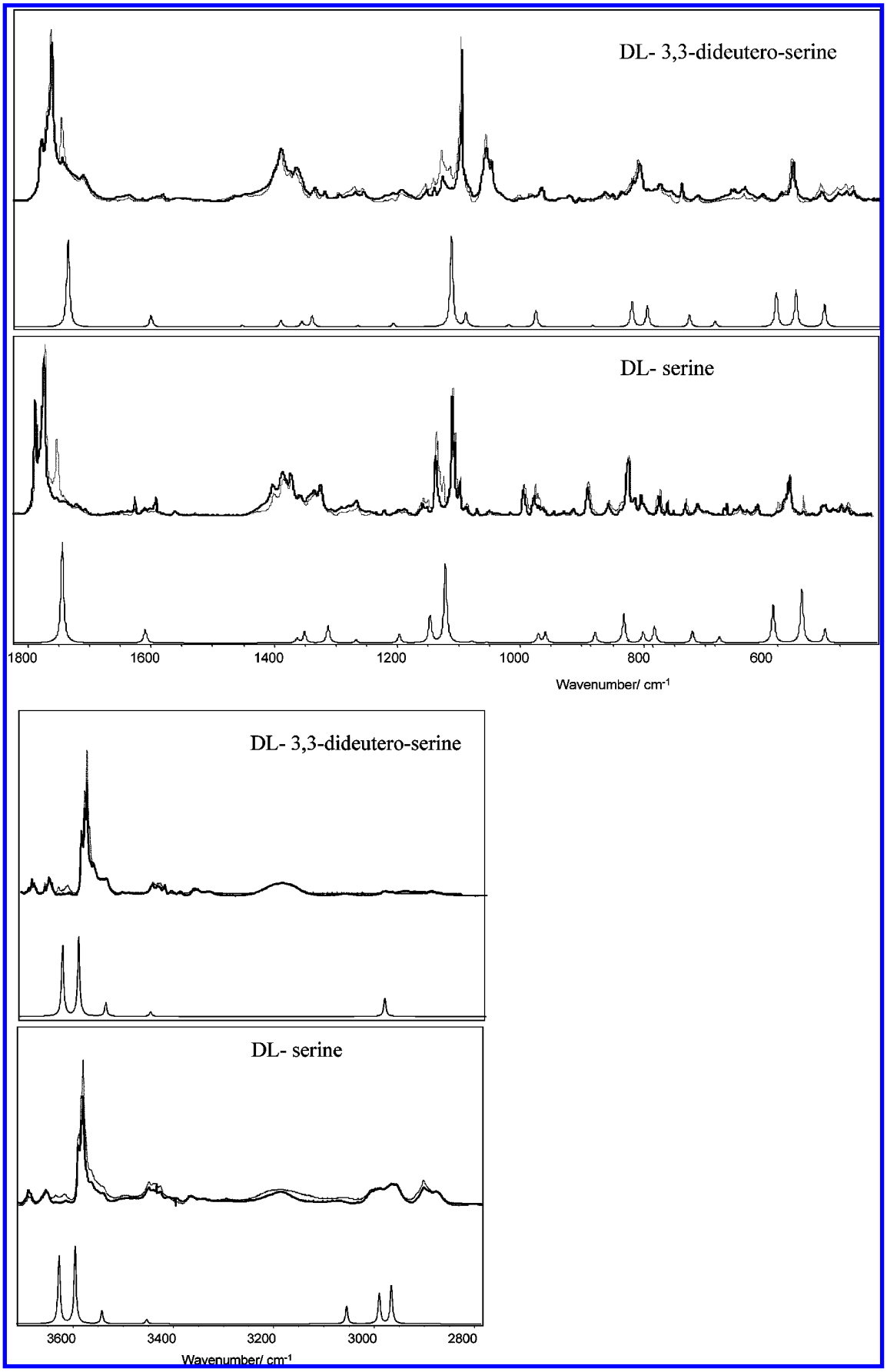

Figure 8. Experimental IR spectra of D,L-serine and D,L-3,3-dideutero-serine molecules isolated in an argon matrix [as deposited (dotted) and after UV irradiation (solid line)] versus DFT/B3LYP/6-311++G(d,p) calculated spectra for conformer **7**, the conformer which decarboxylates faster upon irradiation. (a) 1800−400 cm^{-1} region; (b) 3700−2800 cm^{-1} region.

analysis of the spectrum of the latter molecule. The spectrum of the deuterated isotopologue is dominated by bands due to conformer **1**. In similarity to the spectrum of the nondeuterated serine, the intense (but disappearing upon UV irradiation of the matrix) band due to $\nu C-O_C$ vibration of conformer **7** is clearly observed at 1124 cm^{-1}.

It is also interesting to note that ethanolamine was found to absorb at ca. 1035 cm^{-1} ($\nu N-C$ [57,60,61]). The DFT/B3LYP/6-311++G(d,p) calculations for deuterated ethanolamine also predicted a medium intensity IR band at this frequency. In the spectrum of nondeuterated serine, there are relatively intense bands at ca. 1035 cm^{-1} and in the spectrum of the irradiated matrix no band due to photoproduced ethanolamine could be clearly observed in this region. However, in the less congested spectrum of deuterated serine, a new band around 1035 cm^{-1} could be noticed, providing further evidence of photoproduction of ethanolamine during UV irradiation of serine.

Region Below 900 cm^{-1}. The most intense bands predicted by calculations below 900 cm^{-1} are due to $\tau C-O_C$ torsional mode in all conformers and due to the ωNH_2 wagging and $\tau C-O_A$ modes of **A** and **C** conformers. For conformers **B**, the $\tau C-O_A$ bands are predicted at frequencies below 400 cm^{-1} (out of the studied spectral region), whereas the low-intensity ωNH_2 bands should appear at ca. 920−940 cm^{-1}. The exception is conformer **3**, where $\tau C-O_A$ band was predicted to occur at 590 cm^{-1} (at the highest frequency of all conformers, due to the involvement of the alcohol group in the strongest H-bond interaction among all the nine experimentally observed conformers) and where ωNH_2 vibration was predicted to give rise to absorption at 824 cm^{-1}, at nearly the same frequency as in conformers **A** and **C** (see Tables S3−S21).

Accordingly to the calculations, the intense group of bands observed at ca. 820 cm^{-1} for both deuterated and nondeuterated serine is ascribed mainly to the ωNH_2 wagging vibrations with predicted frequencies in this range. On the other hand, the $\tau C-O_A$ torsions with predicted frequencies in this region, correspond to OH_A groups involved in H-bonding. Such vibrations could be expected to give rise to considerably broad bands that are difficult to be experimentally detected. Indeed, in the experimental spectra, it was not possible to clearly identify the bands due to these modes in both the deuterated and nondeuterated species. A similar situation was in fact also noticed in the case of the expected bands due to the $\tau C-O_C$ torsion in **B** conformers, where the carboxyl group is also involved in a strong H bond, which could not be either experimentally observed. However, the bands due to this mode in **A** and **C** conformers, where the OH_C group is not taking part in H bonding, are clearly observed experimentally. For nondeuterated serine, the band at 579 cm^{-1}, which almost disappears upon irradiation, is ascribed to the **C**-type conformer **7** (calculated frequency 594 cm^{-1}), whereas the **A** conformers give rise to the intense doublet at 568/566 cm^{-1} (conformers **1** and **6**; predicted at 582 and 586 cm^{-1}) and 617 cm^{-1} (conformer **4**; predicted at 625 cm^{-1}). A similar pattern was also found for DL-3,3-dideutero-serine (see Table 4).

Conformational Selectivity of the UV Induced Decarboxylation. Its Relevance to Identification of the C Conformer. As already mentioned, the observed photodecarboxylation of serine shows a clear dependence on the conformation of the carboxylic group. The photochemical CO_2 evolution occurred preferentially for those conformers where the carboxylic group is cis and is not acting as proton donor. The **C** conformer reacts faster, followed by **A**-type conformers, whereas **B** conformers react considerably slower. The different rates of decarboxylation associated with the three groups of serine conformers strongly facilitated the assignment of the experimental spectra. In particular, this photoeffect enabled an easy identification of the **C**-type conformer **7**, which had never been observed previously. The spectra of serine and deuterated serine, recorded before and after UV irradiation, are presented in Figure 8. These experimental spectra are compared with the theoretical spectra calculated for C-type conformers **7** of both isotopologues. As can be seen in Figure 8, the identification of the **C** conformer is particularly clear in the case of the deuterated compound, where a larger number of vibrations originated in this form appear in weakly congested spectral regions.

Conclusions

Extensive conformational analysis has been performed for the molecule of serine. The conformers, identified on the basis of geometry optimizations carried out at the DFT/B3LYP/6-311++G(d,p) level, were classified into 12 groups, according to an intramolecular hydrogen bonding pattern. Comparison of the IR spectra calculated for nine most stable conformers of serine with experimental spectrum of monomers of the compound isolated in low-temperature Ar matrix led to the conclusion that all nine conformers are populated in inert-gas matrixes. Analysis of the experimental IR spectra in terms of coexistence of different groups of conformers frozen in a matrix was significantly facilitated by the effects of UV irradiation and annealing of the solid argon matrix. Upon UV (λ > 200 nm) irradiation, serine underwent photodecarboxylation. Efficiency of this process depended on the conformational structure adopted by the conformers. Also effects of annealing of the matrix were different for different groups of conformers. This allowed grouping of the observed IR bands and their assignment to particular types of conformers or to individual conformers. The conclusions derived from the study of serine were reinforced by the results of the analogous investigation carried out for 3,3-dideutero serine.

Acknowledgment. This work was financially supported by "Fundação para a Ciência e a Tecnologia" (FCT, Project POCTI/QUI/59019/2004), Lisbon, and GRICES (Project 00813). S.J. acknowledges the FCT Grant SFRH/BD/6696/2001. Computational support was provided by the Ohio Supercomputer Center. P.R.C. gratefully acknowledges support from the NIH.

Supporting Information Available: Figure S1 and Tables S1−S22. This material is available free of charge via the Internet at http://pubs.acs.org.

References and Notes

(1) Oró, J. *Nature* **1961**, *190*, 389. Chyba, C. F.; Thomas, P. J.; Brookshaw L.; Sagan, C. *Science* **1990**, *249*, 366.
(2) Bernstein, M. P.; Sandford, S. A.; Allamandola, L. J. *Sci. Am.* **1999**, *281*, 42.
(3) Kuan, Y. J.; Charnley, S. B.; Huang, H. C.; Tseng, W. L.; Kisiel, Z. *Astrophys. J.* **2003**, *593*, 848.
(4) Kuan, Y. J.; Charnley, S. B.; Huang, H. C.; Kisiel, Z.; Ehrenfreund, P.; Tseng, W. L.; Yan, C. H. *Adv. Space Res.* **2004**, *33*, 31.
(5) Kuan, Y. J.; Huang, H. C.; Charnley, S. B.; Tseng, W. L.; Snyder, L. E.; Ehrenfreund, P.; Kisiel, Z.; Thorwirth, S.; Bohn, R. K.; Wilson, T. L. *Bioastron. 2002: Live Among the Stars − IAU Symp.* **2004**, *213*, 185.
(6) Gómez-Zavaglia, A.; Fausto, R. *Phys. Chem. Chem. Phys.* **2003**, *5*, 3154.
(7) Suenram R. D.; Lovas, F. J. *J. Mol. Spectrosc.* **1978**, *72*, 372.
(8) Suenram, R. D.; Lovas, F. J. *J. Am. Chem. Soc.* **1980**, *102*, 7180.
(9) Iijima, K.; Tanaka, K.; Onuma, S. *J. Mol. Struct.* **1991**, *246*, 257.
(10) Iijima, K.; Beagley, B. *J. Mol. Struct.* **1991**, *248*, 133.
(11) Rosado, M. T. S.; Duarte, M. L. T. S.; Fausto, R. *J. Mol. Struct.* **1997**, *410*, 343.

(12) Stepanian, S. G.; Reva, I. D.; Radchenko, E. D.; Rosado, M. T. S.; Duarte, M. L. T. S.; Fausto, R.; Adamowicz, L. *J. Phys. Chem.* **1998**, *102*, 1041.
(13) Stepanian, S. G.; Reva, I. D.; Radchenko, E. D.; Adamowicz, L. *J. Phys. Chem.* **2001**, *105A*, 10664.
(14) Rosado, M. T. S. *Estrutura Molecular e Espectros Vibracionais de n- e α-Aminoácidos Simples*, Ph.D. Thesis, University of Lisbon, Portugal, 2004.
(15) Kikuchi, O.; Natsui, T.; Kozaki, T. *J. Mol. Struct. (THEOCHEM)* **1990**, *207*, 103.
(16) Ding, Y.; Krogh-Jespersen, K. *Chem. Phys. Lett.* **1992**, *199*, 261.
(17) Dixon, D. A.; Lipscomb, W. N. *J. Biol. Chem.* **1976**, *251*, 5992.
(18) Clementi, E.; Cavallone, F.; Scordamaglia, R. *J. Am. Chem. Soc.* **1997**, *99*, 5531.
(19) Wright, L. R.; Borkman, R. F. *J. Am. Chem. Soc.* **1980**, *102*, 6207.
(20) Alsenoy, C. V.; Scarsdale, J. N.; Sellers, H. L.; Schäfer, L. *Chem. Phys. Lett.* **1981**, *80*, 124.
(21) Espinosa-Muller, A. W.; Bravo, A. N. *J. Mol. Struct. (THEOCHEM)* **1982**, *90*, 203.
(22) Masamura, M. *J. Mol. Struct. (THEOCHEM)* **1987**, *152*, 293.
(23) Alsenoy, C. V.; Kulp, S.; Siam, K.; Klimkowski, V. J.; Ewbank, J. D.; Schäfer, L. *J. Mol. Struct. (THEOCHEM)* **1988**, *181*, 169.
(24) Masamura, M. *J. Mol. Struct. (THEOCHEM)* **1988**, *164*, 299.
(25) Tarakeshwar, P.; Manogaran, S. *J. Mol. Struct. (THEOCHEM)* **1994**, *305*, 205.
(26) Tortonda, F. R.; Silla, E.; Tunón, I.; Rinaldi, D.; Ruiz-López, M. F. *Theor. Chem. Acc.* **2000**, *104*, 89.
(27) Noguera, M.; Rodríguez-Santiago, L.; Sodupe, M.; Bertran, J. *J. Mol. Struct. (THEOCHEM)* **2001**, *537*, 307.
(28) Lakard, B. *J. Mol. Struct. (THEOCHEM)* **2004**, *681*, 183.
(29) Lambie, B.; Ramaekers, R.; Maes, G. *J. Phys. Chem.* **2004**, *108A*, 10426.
(30) Gronert, S.; O'Hair, R. A. J. *J. Am. Chem. Soc.* **1995**, *117*, 2071.
(31) Pierazzo, E.; Chyba, C. F. *Meteorit. Planet. Sci.* **1999**, *34*, 909.
(32) Blank, J. G.; Miller, G. H.; Ahrens, M. J.; Winans, R. E. *Origin Life Evol. Biosphere* **2001**, *31*, 15.
(33) Ehrenfreund, P.; Bernstein, M. P.; Dworkin, J. P.; Sandford, S. A.; Allamandola, L. J. *Astrophys. J.* **2001**, *550*, L95.
(34) Zubavichus, Y.; Fuchs, O.; Weinhardt, L.; Heske, C.; Umbach, E.; Denlinger, J. D.; Grunze, M. *Radiat. Res.* **2004**, *161*, 346.
(35) Sato, N.; Quitain, A. T.; Kang, K.; Daimon, H.; Fujie, K. *Ind. Eng. Chem. Res.* **2004**, *43*, 3217.
(36) Jarmelo, S.; Lapinski, L.; Fausto, R. *Proceedings of the Annual Meeting of the Cryobiology and Low Temperature Biology Societies: Cryobiomol 2003*, From the Low-Temperature Physics and Chemistry of Biological Molecules to Life in Extreme Low-Temperature Conditions, Coimbra, Portugal, 2003; p 142.
(37) Jarmelo, S.; Lapinski, L.; Nowak, M. J.; Fausto, R. *Proceedings of the XX IUPAC Symposium on Photochemistry*, Granada, Spain, 2004; p 355.
(38) Szczesniak, M.; Nowak, M. J.; Rostkowska, H.; Szczepaniak, K.; Person, W. B.; Shugar, D. *J. Am. Chem. Soc.* **1983**, *105*, 5969.
(39) Frisch, M. J.; Trucks, G. W.; Schlegel, H. B.; Scuseria, G. E.; Robb, M. A.; Cheeseman, J. R.; Zakrzewski, V. G.; Montgomery, J. A., Jr.; Stratmann, R. E.; Burant, J. C.; Dapprich, S.; Millam, J. M.; Daniels, A. D.; Kudin, K. N.; Strain, M. C.; Farkas, O.; Tomasi, J.; Barone, V.; Cossi, M.; Cammi, R.; Mennucci, B.; Pomelli, C.; Adamo, C.; Clifford, S.; Ochterski, J.; Petersson, G. A.; Ayala, P. Y.; Cui, Q.; Morokuma, K.; Malick, D. K.; Rabuck, A. D.; Raghavachari, K.; Foresman, J. B.; Cioslowski, J.; Ortiz, J. V.; Stefanov, B. B.; Liu, G.; Liashenko, A.; Piskorz, P.; Komaromi, I.; Gomperts, R.; Martin, R. L.; Fox, D. J.; Keith, T.; Al-Laham, M. A.; Peng, C. Y.; Nanayakkara, A.; Gonzalez, C.; Challacombe, M.; Gill, P. M. W.; Johnson, B. G.; Chen, W.; Wong, M. W.; Andres, J. L.; Head-Gordon, M.; Replogle, E. S.; Pople, J. A. *Gaussian 98*, revision A.9; Gaussian, Inc.: Pittsburgh, PA, 1998.
(40) Binkley, J. S.; Pople, J. A.; Hehre, W. J. *J. Am. Chem. Soc.* **1980**, *102*, 939.
(41) Pietro, W. J.; Francl, M. M.; Hehre, W. J.; Defrees, D. J.; Pople, J. A.; Binkley, J. S. *J. Am. Chem. Soc.* **1982**, *104*, 5039.
(42) Frisch, M. J.; Pople, J. A.; Binkley, J. S. *J. Chem. Phys.* **1984**, *80*, 3265.
(43) McLean, A. D.; Chandler, G. S. *J. Chem. Phys.* **1980**, *72*, 5639.
(44) Becke, A. D. *Phys. Rev.* **1988**, *38A*, 3098.
(45) Lee, C. T.; Yang, W. T.; Parr, R. G. *Phys. Rev.* **1988**, *37B*, 785.
(46) Gómez-Zavaglia, A.; Fausto, R. *Vibrat. Spectrosc.* **2003**, *33*, 105.
(47) Borba, A.; Gómez-Zavaglia, A.; Lapinski, L.; Fausto, R. *Phys. Chem. Chem. Phys.* **2004**, *6*, 2101.
(48) De Frees, D.; McLean, A. *J. Chem. Phys.* **1985**, *82*, 333.
(49) Stepanian, S. G.; Reva, I. D.; Radchenko, E. D.; Adamowicz, L. *J. Phys. Chem.* **1998**, *102A*, 4623.
(50) Reva, I. D.; Stepanian, S. G.; Adamowicz, L.; Fausto, R. *J. Phys. Chem.* **2001**, *105A*, 4773.
(51) Császár, A. G. *J. Am. Chem. Soc.* **1992**, *114*, 9568.
(52) Owen, N. L.; Sheppard, N. *Proc. Chem. Soc., London* **1963**, 264.
(53) Piercy, J. E.; Subrahmanyan, S. V. *J. Chem. Phys.* **1965**, *42*, 1475.
(54) Bayley, J.; North, A. M. *Trans. Faraday Soc.* **1968**, *64*, 1499.
(55) Fausto, R.; Teixeira-Dias, J. J. C. *J. Mol. Struct. (THEOCHEM)* **1987**, *150*, 381.
(56) Svensson, T.; Nelander, B.; Karlström, G. *Chem. Phys.* **2001**, *265*, 323.
(57) Cacela, C.; Duarte, M. L.; Fausto, R. *J. Mol. Struct.* **1999**, *482/483*, 591.
(58) Fausto, R.; Batista de Carvalho, L. A. E.; Teixeira-Dias, J. J. C.; Ramos, M. N. *J. Chem. Soc. Faraday Trans.* 2 **1989**, *85*, 1945.
(59) Jarmelo, S.; Maiti, N.; Anderson, V.; Carey, P.; Fausto, R. *J. Phys. Chem.* **2005**, *109A*, 2069.
(60) Räsänen, M.; Aspiala, A.; Homanen, L.; Murto, J. *J. Mol. Struct.* **1982**, *96*, 81.
(61) EPA Vapor Phase Library, CAS Number 141-43-5, 2001 Thermo Galactic.
(62) Jarmelo, S.; Fausto, R. *Phys. Chem. Chem. Phys.* **2002**, *4*, 1555.